AD-A172 231 LINEAR AND NONLINEAR THEORY OF THE DOPPLER-SHIFTED CYCLOTRON RESONANCE MA..(U) NAVAL RESEARCH LAB WASHINGTON DC A W FLIFLET 29 AUG 86 NRL-MR-5812 1/1

UNCLASSIFIED F/G 20/5 NL

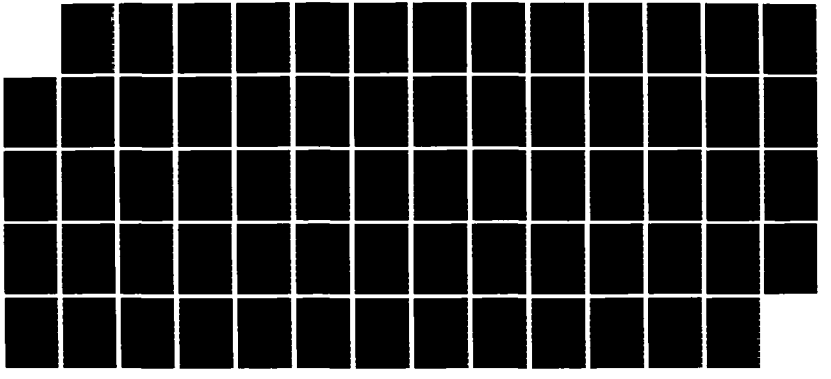

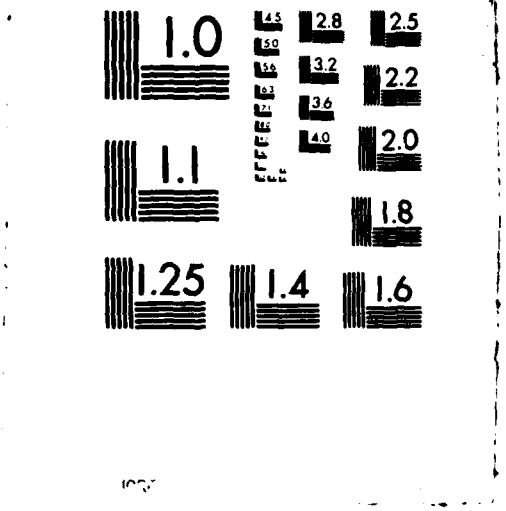
1.0
1.1
1.25
1.4
1.6
1.8
2.0
2.2
2.5
2.8
3.2
3.6
4.0

Linear and Nonlinear Theory of the Doppler-Shifted Cyclotron Resonance Maser Based on TE and TM Waveguide Modes

ARNE W. FLIFLET

High Power Electromagnetic Radiation Branch
Plasma Physics Division

SECURITY CLASSIFICATION OF THIS PAGE

AD-A172 231

REPORT DOCUMENTATION PAGE

1a. REPORT SECURITY CLASSIFICATION UNCLASSIFIED	1b. RESTRICTIVE MARKINGS
2a. SECURITY CLASSIFICATION AUTHORITY	3. DISTRIBUTION / AVAILABILITY OF REPORT Approved for public release; distribution unlimited.
2b. DECLASSIFICATION / DOWNGRADING SCHEDULE	
4. PERFORMING ORGANIZATION REPORT NUMBER(S) NRL Memorandum Report 5812	5. MONITORING ORGANIZATION REPORT NUMBER(S)
6a. NAME OF PERFORMING ORGANIZATION Naval Research Laboratory 6b. OFFICE SYMBOL (If applicable) Code 4740	7a. NAME OF MONITORING ORGANIZATION
6c. ADDRESS (City, State, and ZIP Code) Washington, DC 20375-5000	7b. ADDRESS (City, State, and ZIP Code)
8a. NAME OF FUNDING / SPONSORING ORGANIZATION Office of Naval Research 8b. OFFICE SYMBOL (If applicable)	9. PROCUREMENT INSTRUMENT IDENTIFICATION NUMBER
8c. ADDRESS (City, State, and ZIP Code) Arlington, VA 22217	10. SOURCE OF FUNDING NUMBERS PROGRAM ELEMENT NO. 61153N; PROJECT NO. DN880-061; TASK NO. RR011-09-41; WORK UNIT ACCESSION NO 47-0866-00
11. TITLE (Include Security Classification) Linear and Nonlinear Theory of the Doppler-Shifted Cyclotron Resonance Maser Based on TE and TM Waveguide Modes (U)	
12. PERSONAL AUTHOR(S) Fliflet, Arne W.	
13a. TYPE OF REPORT Interim 13b. TIME COVERED FROM 1/85 TO 3/86	14. DATE OF REPORT (Year, Month, Day) 1986 August 29 15. PAGE COUNT 67
16. SUPPLEMENTARY NOTATION	

17. COSATI CODES		
FIELD	GROUP	SUB-GROUP

18. SUBJECT TERMS (Continue on reverse if necessary and identify by block number)
Cyclotron resonance maser, Circular waveguide
Kinetic theory, Relativistic electron energy
(Continue on page ii)

19. ABSTRACT (Continue on reverse if necessary and identify by block number)

This paper presents a comprehensive theory of the Cyclotron Resonance Maser (CRM) interaction in a circular waveguide. The kinetic theory is used to derive the dispersion relationships for both TE and TM modes. The TE mode case has been investigated by several authors, but there has been comparatively little work on the TM mode case. However, the TM mode interaction competes effectively with the TE mode interaction at relativistic electron energies. The conditions for maximum temporal and spatial growth rates are shown. The TM mode growth rates are found to vanish when the RF wave group velocity equals the beam axial velocity ("grazing incidence"). The single particle theory is used to derive a compact set of self-consistent nonlinear equations for the TE and TM mode interactions. These equations are particularly appropriate for the Cyclotron Auto-Resonance Maser (CARM) regime but applicability extends to other regimes as well. The conditions for optimum efficiency are investigated for oscillator and amplifier configurations at the fundamental and low order harmonic interactions. In the case of a beam with delta function distributions in position and momentum the single particle results in the small signal limit are shown to be equivalent to the kinetic theory results. Design parameters are given for high power amplifier and oscillator configurations.

20. DISTRIBUTION / AVAILABILITY OF ABSTRACT	21. ABSTRACT SECURITY CLASSIFICATION	
☐ UNCLASSIFIED/UNLIMITED ☐ SAME AS RPT. ☒ DTIC USERS	UNCLASSIFIED	
22a. NAME OF RESPONSIBLE INDIVIDUAL Arne W. Fliflet	22b. TELEPHONE (Include Area Code) 202-767-2469	22c. OFFICE SYMBOL Code 4740

DD FORM 1473, 84 MAR — 83 APR edition may be used until exhausted. All other editions are obsolete. — SECURITY CLASSIFICATION OF THIS PAGE

18. SUBJECT TERMS (Continue on reverse if necessary and identify by block number)

Temporal and spatial growth rate
Beam axial velocity
Amplifier
RF wave group velocity
Oscillator

CONTENTS

LINEAR AND NONLINEAR THEORY OF THE DOPPLER-SHIFTED CYCLOTRON RESONANCE MASER BASED ON TE AND TM WAVEGUIDE MODES

I. Introduction

During the past twenty years the fast-wave Cyclotron Resonance Maser (CRM) has been the subject of considerable interest as an efficient, high power source of millimeter-wave radiation. The versatility of the interaction is evidenced by the variety of device concepts which have been developed, including gyrotron oscillators and ampifiers, gyro-klystrons, and high-harmonic gyrotrons. In these devices the radiation frequency is close to the cyclotron frequency or a harmonic and the beam energy is in the weakly relativistic regime. The application of the CRM interaction to higher energy beams and to the generation of higher frequency radiation has led to interest in configurations based on the doppler-shifted CRM interaction. Potential advantages of such configurations include a reduced magnetic field requirement, larger transverse dimensions of the circuit, reduced electron beam pitch angle, high efficiency of order 25%, and increased output power from operation at high voltage.

The theory of the CRM is quite well developed for the weakly relativistic gyrotron regime but the relativistic doppler-shifted regime has received less attention. The theoretical approaches used most often are the kinetic theory based on the linearized Vlasov equation and the single particle theory. The former leads to dispersion equations for the interaction and linear growth

Manuscript approved May 28, 1986.

rates or threshold currents. The latter leads to both linear and nonlinear results for the interaction parameters. The advantage of the kinetic theory is that it can treat more general beam distributions and usually involves fewer a priori assumptions than the single particle method. In addition to providing the saturated efficiency, the single particle theory can be reduced to a compact set of equations useful for scaling studies.

This paper presents a comprehensive theory of the Cyclotron Resonance Maser (CRM) interaction in a waveguide. The circular waveguide geometry was chosen because it corresponds to the experimental geometry most often used at present. The kinetic theory is used to derive the dispersion relationships for both TE and TM modes. The TE mode case has been investigated by several authors, but there has been comparatively little work on the TM mode case. However, the TM mode interaction competes effectively with the TE mode interaction at relativistic electron energies. The conditions for maximum temporal and spatial growth rates are shown. The TM mode growth rates are found to vanish when the RF wave group velocity equals the beam axial velocity ("grazing incidence").

The single particle theory is used to derive a compact set of self-consistent nonlinear equations for the TE and TM mode interactions. These equations are particularly appropriate for the Cyclotron Auto-Resonance Maser (CARM) regime but applicability extends to other regimes as well. The conditions for optimum efficiency are investigated for oscillator and amplifier configurations at the fundamental and low order harmonic interactions. In the case of a beam with delta function distributions in position and momentum the single particle results in the small signal limit are shown to be equivalent to the kinetic theory results.

There is an extensive literature on the theory of Cyclotron Resonance Masers and an exhaustive review will not be attempted. The initial theoretical work on the radiation amplification mechanism was presented independently by Twiss (1958), Schneider (1959) and Gaponov (1959). A single particle theory applicable to the gyrotron configuration was given in an early review by Gaponov et al (1967). An early application of the kinetic theory was carried out by Ott and Manheimer (1975) for a planar configuration. A nonlinear single particle theory for the planar configuration was developed by Sprangle and Manheimer (1975) and further investigated by Sprangle and Drobot (1977). Application of the kinetic theory to TE modes in cylindrical waveguides was given by Chu et al (1980). The TE and TM mode interactions have been considered for a beam with axicentered orbits by Lau (1982). A theory of ultrarelativistic cyclotron self-resonance masers was given by Petelin (1973). The single particle theory of CARM amplifiers and oscillators has been reviewed by Bratman et al (1981,1983). A theory of doppler shifted relativistic CRM amplifiers has been given by Ginzburg et al (1981). Doppler shifted CRM oscillator configurations have been investigated by Kanavets and Klimov (1975) and by Vomvoridis (1982). The excitation of TM modes in CRM oscillators has been investigated by Abubakirov (1983). An induced resonance electron cyclotron (IREC) quasi-optical maser has been investigated by Sprangle et al (1985). Simulation studies of the CARM amplifier have been carried out by Lin (1984) and by Lin and Lin (1985).

The equations and results presented in this paper should provide a useful starting point for developing device concepts based on the doppler-shifted cyclotron maser interaction and for interpreting on going experiments. Although aspects of the present work have been treated

previously, this work extends previous analyses by treating TE and TM modes on an equal footing, considering arbitrary mode indicies and beam guiding center radius, and harmonic number. In addition, derivations of these theoretical results are not generally available. Finally, this work provides a starting point for cosidering more complicated systems such as plasma filled waveguides.

II. Dispersion Relationships from Kinetic Theory

The present analysis considers an electron beam drifting in a vacuum waveguide with an applied axial magnetic field. Dispersion relationships for TE and TM modes in a circular waveguide are derived using linearized Vlasov theory. The derivation follows the approach of Chu and Dialetis (1985) in analyzing the gyromagnetron. The calculation assumes the electron beam current density is sufficiently low to neglect self-fields. The calculation is based on the linearized Vlasov equation

$$\frac{df_1(\vec{r},\vec{p},t)}{dt} = e\,(\vec{E} + \vec{v} \times \vec{B}) \cdot \vec{\nabla}_{\vec{p}}\, f_o(\vec{r},\vec{p},t) \qquad \text{(II.1)}$$

where f_o is the unperturbed distribution function to be constructed from constants of the motion in an applied axial magnetic field, and $\vec{E}$ and $\vec{B}$ are the vacuum waveguide rf fields. The transverse components are given by

$$\vec{E}_t(\vec{r},t) = \mathrm{Re}\{\Pi(z)\vec{e}(\vec{r})e^{-i\omega t}\} \qquad \text{(II.2a)}$$

$$\vec{B}_t(\vec{r},t) = \mathrm{Re}\{T(z)\vec{b}(\vec{r})e^{-i\omega t}\} \qquad \text{(II.2b)}$$

where $\vec{e}$ and $\vec{b}$ are transverse vector functions given by

$$\vec{e} = \hat{z} \times \vec{\nabla}_t \psi \qquad \text{(II.3a)}$$

$$\vec{b} = -\vec{\nabla}_t \psi \qquad \text{(II.3b)}$$

for a TE mode, and by

$$\vec{e} = -\vec{\nabla}_t \psi \qquad \text{(II.4a)}$$

$$\vec{b} = -\hat{z} \times \vec{\nabla}_t \psi \qquad \text{(II.4b)}$$

for a TM mode. The scalar function ψ satisfies the Helmholtz equation

$$(\nabla_t^2 + k_t^2)\psi = 0 \qquad \text{(II.5)}$$

and the boundary condition

$$\frac{\partial \psi}{\partial n} = 0 \qquad \text{(II.6)}$$

on the waveguide boundary for a TE mode, or the boundary condition

$$\psi = 0 \qquad \text{(II.7)}$$

at the waveguide boundary for a TM mode. In Eq. (II.5) k_t denotes the transverse wavenumber and in Eq.(II.6) $\partial/\partial n$ denotes the normal derivative.

The vector functions satisfy the following orthonormality condition when integrated over the waveguide cross section:

$$\int_S ds \ \vec{h}_i \cdot \vec{h}_j = \delta_{ij} \tag{II.8}$$

where $\vec{h}$ denotes either $\vec{e}$ or $\vec{b}$ and $\delta_{ij} = 1$ if $i=j$, $\delta_{ij} = 0$ if $i \neq j$. The axial field components are given by

$$B_z = \mathrm{Re}\{i\frac{k_t^2}{\omega}\Pi(z)\psi e^{-i\omega t}\} \tag{II.9}$$

for a TE mode, and by

$$E_z = \mathrm{Re}\{i\frac{c^2 k_t^2}{\omega} T(z)\psi e^{-i\omega t}\} \tag{II.10}$$

for a TM mode. The axial profile functions $\Pi(z)$ and $T(z)$ are related according to

$$T(z) = -\frac{i}{\omega}\frac{d\Pi(z)}{dz} \tag{II.11}$$

for a TE mode and

$$\Pi(z) = -\frac{ic^2}{\omega}\frac{dT(z)}{dz} \tag{II.12}$$

for a TM mode. In the case of a circular waveguide, the scalar function ψ is given by

$$\psi_{mn}(\vec{r}) = C_{mn}J_{mn}(k_{mn}r)e^{im\theta} \tag{II.13}$$

where J_m is a Bessel function of the first kind and $k_{mn} = x_{mn}/r_w$. x_{mn} is the nth zero of J_m' (prime denotes differentiation) for a TE mode or the nth zero of J_m for a TM mode, and r_w is the waveguide wall radius. The normalization constant is given by

$$C_{mn} = \{[\pi(x_{mn}^2 - m^2)]^{1/2}J_m(x_{mn})\}^{-1} \tag{II.14}$$

for a TE mode and by

$$C_{mn} = \{\sqrt{\pi}\, x_{mn}J_m'(x_{mn})\}^{-1} \tag{II.15}$$

for a TM mode.

To evaluate the RHS of Eq.(II.1), the unit vectors $\vec{e}_t = \vec{p}_t/|\vec{p}_t|$ and $\vec{e}_\phi = \vec{e}_t \times \vec{e}_z$ are introduced. In terms of the notation of Fig. 1, these unit vectors satisfy the relationships

$$\vec{e}_t = \cos(\phi-\theta)\vec{e}_r + \sin(\phi-\theta)\vec{e}_\theta \tag{II.16a}$$

$$\vec{e}_\phi = -\sin(\phi-\theta)\vec{e}_r + \cos(\phi-\theta)\vec{e}_\theta \tag{II.16b}$$

Using these unit vectors in Eq.(II.1) leads to

$$\begin{aligned}\frac{df_1}{dt} = e\{&E_r\cos(\phi-\theta) + E_\theta\sin(\phi-\theta) + \frac{p_z}{\gamma m_o}[B_r\sin(\phi-\theta) - B_\theta\cos(\phi-\theta)]\}\frac{\partial f_o}{\partial p_t} \\ &+ \frac{ep_t}{\gamma m_o}\{B_\theta\cos(\phi-\theta) - B_r\sin(\phi-\theta)\}\frac{\partial f_o}{\partial p_z} \\ &+e\{-E_r\sin(\phi-\theta) + E_\theta\cos(\phi-\theta) + \frac{p_z}{\gamma m_o}[B_\theta\sin(\phi-\theta) + B_r\cos(\phi-\theta)] \\ &-B_z\frac{p_t}{\gamma m_o}\}\frac{1}{p_t}\frac{\partial f_o}{\partial \phi}\end{aligned} \tag{II.17}$$

for a TE mode and a similar expression for a TM mode. Using Graf's addition theorem (Abramowitz and Stegun 1964), and considering the interaction with a forward propagating wave ($\Pi(z) = \Pi_o\exp(ik_z z)$), the expressions in brackets in Eq.(II.17) can be rewritten as:

$$E_r^+\cos(\phi-\theta) + E_\theta^+\sin(\phi-\theta) = \mathrm{Re}\{\Pi_o C_{mn} k_{mn} e^{-i(\omega t - k_z z - m\theta + m\frac{\pi}{2})} \sum_q J_q(k_{mn} r_o)$$

$$J'_{m+q}(k_{mn} r_L) e^{iq\tilde{\phi}}\} \qquad \text{(II.18a)}$$

$$-E_r^+\sin(\phi-\theta) + E_\theta^+\cos(\phi-\theta) = \mathrm{Re}\{i\Pi_o C_{mn} k_{mn} e^{-i(\omega t - k_z z - m\theta + m\frac{\pi}{2})}$$

$$\sum_q \frac{m+q}{k_{mn} r_L} J_q(k_{mn} r_o) J_{m+q}(k_{mn} r_L) e^{iq\tilde{\phi}}\} \qquad \text{(II.18b)}$$

$$B_r^+\sin(\phi-\theta) - B_\theta^+\cos(\phi-\theta) = \mathrm{Re}\{-\frac{k_z}{\omega} \Pi_o C_{mn} k_{mn} e^{-i(\omega t - k_z z - m\theta + m\frac{\pi}{2})}$$

$$\sum_q J_q(k_{mn} r_o)\ J'_{m+q}(k_{mn} r_L) e^{iq\tilde{\phi}}\} \qquad \text{(II.18c)}$$

$$B_\theta^+\sin(\phi-\theta) + B_r^+\cos(\phi-\theta) = \mathrm{Re}\{-\frac{ik_z}{\omega} \Pi_o C_{mn} k_{mn} e^{-i(\omega t - k_z z - m\theta + m\frac{\pi}{2})}$$

$$\sum_q \frac{m+q}{k_{mn} r_L} J_q(k_{mn} r_o) J_{m+q}(k_{mn} r_L)\ e^{iq\tilde{\phi}}\} \qquad \text{(II.18d)}$$

$$B_z = \mathrm{Re}\{i\frac{k_{mn}}{\omega} \Pi_o C_{mn} k_{mn} e^{-i(\omega t - k_z z - m\theta + m\frac{\pi}{2})}$$

$$\sum_q J_q(k_{mn} r_o)\ J_{m+q}(k_{mn} r_L)\ e^{iq\tilde{\phi}}\} \qquad \text{(II.18e)}$$

The unperturbed distribution function f_o is now treated as a function of r_o, p_t and p_z and the partial derivatives are written as

$$\frac{\partial f_o}{\partial p_t} = \frac{\partial f_o}{\partial p_t} + \frac{1}{m_o \Omega_e}(e^{i\tilde{\phi}} + e^{-i\tilde{\phi}}) \frac{\partial f_o}{\partial r_o} \tag{II.19a}$$

$$\frac{1}{p_t}\frac{\partial f_o}{\partial \phi} = \frac{i}{2m_o \Omega_e} (e^{i\tilde{\phi}} - e^{-i\tilde{\phi}}) \frac{\partial f_o}{\partial r_o} \tag{II.19b}$$

where in the above equations $f_o = f_o(p_z, p_t, \phi)$ on the LHS and $f_o = f_o(p_z, p_t, r_o)$ on the RHS. Substituting Eqs.(II.18) and (II.19) into Eq.(II.17) yields

$$\frac{df_1^+}{dt} = \mathrm{Re}\{\frac{e\Pi_o}{\omega} C_{mn} k_{mn} \sum_s e^{-i(\omega t - k_z z - m\phi - (s-m)\tilde{\phi} + m\frac{\pi}{2})}$$

$$[J_{s-m}(k_{mn} r_o)\, J'_s(k_{mn} r_L)\, [(\omega - \frac{k_z p_z}{\gamma m_o}) \frac{\partial f_o}{\partial p_t} + \frac{k_z p_t}{\gamma m_o} \frac{\partial f_o}{\partial p_z}]$$

$$- \frac{1}{m_o \Omega_e} \{J'_{s-m}(k_{mn} r_o) J_s(k_{mn} r_L)\, (\omega - \frac{k_z p_z}{\gamma m_o})$$

$$- \frac{1}{2}[J_{s-m-1}(k_{mn} r_o) J_{s-1}(k_{mn} r_L) - J_{s-m+1}(k_{mn} r_o) J_{s+1}(k_{mn} r_L)]\, \frac{k_{mn} p_t}{\gamma m_o}\, \}\frac{\partial f_o}{\partial r_o}]\} \tag{II.20}$$

In what follows, the the last term on the RHS of Eq.(II.20) involving $\partial f_o / \partial r_o$ will be neglected. It can be shown that for configurations which optimize the Cyclotron Maser interaction, contributions arising from this term are negligible. Instead this term leads to the Peniotron interaction (Döhler et al (1978), Vitello (1984), Zhang (1985)). Eq.(II.20) is easily solved using the method of characteristics (Krall and Trivelpiece 1973) in which the RHS is integrated with respect to time along the unperturbed orbits, i.e., $z(t') = z + v_{zo}(t'-t)$, $\phi(t') = \phi + \Omega_e(t'-t)/\gamma$, $\tilde{\phi}(t') = \tilde{\phi} + \Omega_e(t'-t)/\gamma$. For a TE mode this gives

$$f_{1TE}^{+} = \mathrm{Re}\{e\,\frac{\Pi_o}{\omega}\,C_{mn}k_{mn}\sum_s F_{sm}^{TE}(r_o,p_t,p_z)\,\frac{ie^{-i(\omega t-k_z z-m\phi-(s-m)\bar{\phi}+m\frac{\pi}{2})}}{\omega-k_z v_z-s\Omega_e/\gamma}\} \tag{II.21}$$

where

$$F_{sm}^{TE}(r_o,p_t,p_z) = J_{s-m}(k_{mn}r_o)J_s'(k_{mn}r_L)[(\omega-\frac{k_z p_z}{\gamma m_o})\,\frac{\partial f_o}{\partial p_t}+\frac{k_z p_t}{\gamma m_o}\,\frac{\partial f_o}{\partial p_z}] \tag{II.22}$$

and for a TM mode

$$f_{1TM}^{+} = \mathrm{Re}\{-ecT_oC_{mn}k_{mn}\sum_s F_{sm}^{TM}(r_o,p_t,p_z)\frac{e^{-i(\omega t-k_z z-m\phi-(s-m)\bar{\phi}+m\frac{\pi}{2})}}{\omega-k_z v_z-s\Omega_e/\gamma} \tag{II.23}$$

where

$$F_{sm}^{TM}(r_o,p_t,p_z) = \frac{s}{k_{mn}r_L}J_{s-m}(k_{mn}r_o)J_s(k_{mn}r_L)\,[(\frac{p_z}{\gamma m_o c}-\frac{ck_z}{\omega})\,\frac{\partial f_o}{\partial p_t}+$$

$$(-\frac{1}{\gamma m_o c}+\frac{\omega_{mn}^2 p_t}{s\Omega_e m_o c})\,\frac{\partial f_o}{\partial p_z}] \tag{II.24}$$

In Eq.(II.24) $\omega_{mn} = k_{mn}c$ and Ω_e is the non-relativistic cyclotron frequency.

The dispersion relationships are obtained from Maxwell's Equations. The wave equation for a TE mode in cylindrical symmetry is

$$(\frac{1}{c^2}\,\frac{\partial^2}{\partial t^2}-\nabla^2)B_z = \mu_o[\frac{1}{r}\,\frac{\partial}{\partial r}(rJ_\theta^{(1)})-\frac{1}{r}\,\frac{\partial J_r^{(1)}}{\partial\theta}] \tag{II.25}$$

where the components of the perturbed current density are given by:

$$J_\theta^{(1)} = -e\int d^3p f_1 v_\theta = -e\int d^3p f_1 v_t \sin(\phi-\theta) \tag{II.26a}$$

$$J_r^{(1)} = -e\int d^3p f_1 v_r = -e\int d^3p f_1 v_t \cos(\phi-\theta) \qquad \text{(II.26b)}$$

Similarly, the wave equation for a TM mode is

$$\left(\frac{1}{c^2}\frac{\partial^2}{\partial t^2} - \nabla^2\right) E_z = -\mu_o \frac{\partial J_z^{(1)}}{\partial z} - \frac{1}{\varepsilon_o}\nabla_z \rho^{(1)} \qquad \text{(II.27)}$$

where the perturbed axial current and charge densities are given by:

$$J_z^{(1)} = -e\int d^3p f_1 v_z \qquad \text{(II.28a)}$$

$$\rho^{(1)} = -e\int dp^3 f_1 \qquad \text{(II.28b)}$$

Substituting Eq.(II.9) into Eq.(II.25), multiplying by $rJ_m(k_{mn}r)e^{-im\theta}$ and integrating with respect to r and θ leads to:

$$\frac{\omega^2}{c^2} - k_{mn}^2 - k_z^2 = \frac{2i\omega\mu_o \; e^{-i(k_z z-\omega t)}}{\Pi_o k_{mn}^2 C_{mn}\, 2\pi\, r_w^2\, (1-m^2/x_{mn}^2)\, J_m^2(x_{mn})}$$

$$\int_o^{2\pi} d\theta \int_o^{r_w} r dr J_m(k_{mn}r) e^{-im\theta}\left[\frac{1}{r}\frac{\partial}{\partial r}(rJ_\theta^{(1)}) - \frac{1}{r}\frac{\partial J_r^{(1)}}{\partial \theta}\right] \qquad \text{(II.29)}$$

Integrating the RHS of Eq.(II.29) by parts and applying Graf's addition theorem yields

$$\frac{\omega^2}{c^2} - k_{mn}^2 - k_z^2 = -\frac{e^2\mu_o}{\pi r_w^2 \left(1-\frac{m^2}{x_{mn}^2}\right) J_m^2(x_{mn})} \sum_{s,q} \int r dr d\theta p_t dp_t d\phi dp_z$$

$$iF_{sm}^{TE} v_t e^{i[(s-m-q)\tilde{\phi} - \frac{\pi}{2}]} J_q(k_{mn} r_o) J'_{q+m}(k_{mn} r_L) \tag{II.30}$$

Finally, using the relationship

$$r dr p_t dp_t d\phi d\theta = r_o dr_o p_t dp_t d\tilde{\phi} d\theta \tag{II.31}$$

the dispersion relationship for the TE mode interaction with a given harmonic s is obtained:

$$\frac{\omega^2}{c^2} - k_{mn}^2 - k_z^2 = -\frac{2e^2\mu_o}{r_w^2 \left(1-\frac{m^2}{x_{mn}^2}\right) J_m^2(x_{mn}) m_o} \int r_o dr_o \int_o^\infty dp_t p_t^2 \int_{-\infty}^\infty dp_z$$

$$J_{s-m}(k_{mn} r_o) J'_s(k_{mn} r_L) \frac{F_{sm}^{TE}(r_o, p_t, p_z)}{\gamma(\omega - k_z v_z - s\Omega_e/\gamma)} \tag{II.32}$$

By a similar analysis the dispersion relationship for a TM mode is obtained:

$$\frac{\omega^2}{c^2} - k_{mn} - k_z^2 = -\frac{2e^2\mu_o}{r_w^2 J'^2_m(x_{mn}) m_o} \int r_o dr_o \int_o^\infty dp_t p_t^2 \int_{-\infty}^\infty dp_z \frac{\omega}{s\Omega_e} \frac{s}{k_{mn} r_L}$$

$$J_{s-m}(k_{mn} r_o) J_s(k_{mn} r_L) \frac{\left(\frac{\omega v_z}{c} - k_z c\right) F_{sm}^{TM}(r_o, p_t, p_z)}{(\omega - k_z v_z - s\Omega_e/\gamma)} \tag{II.33}$$

Writing the unperturbed distribution function in the form

$$f_o = \sigma_o h_o(r_o) g_o(p_t, p_z) \tag{II.34}$$

where σ_o is the number of beam electrons per unit volume, and integrating the RHS of Eqs.(II.32) and (II.33) by parts with respect to p_t and p_z, the TE mode equation becomes

$$\frac{\omega^2}{c^2} - k_{mn}^2 - k_z^2 = -\frac{2e^2\mu_o\sigma_o}{m_o r_w^2 K_{mn}} \int r_o dr_o \int_0^\infty p_t dp_t \int_{-\infty}^{\infty} dp_z h_o(r_o) g_o(p_t, p_z)$$

$$\left[\frac{(\omega^2 - k_z^2 c^2)\, p_t^2 H_{sm}}{\gamma^3 m_o^2 c^2 (\omega - k_z v_z - \frac{s\Omega_e}{\gamma})^2} - \frac{(\omega - k_z v_z)\, Q_{sm}}{\gamma(\omega - k_z v_z - \frac{s\Omega_e}{\gamma})}\right] \quad \text{(II.35)}$$

where

$$H_{sm} = J_{s-m}^2(k_{mn} r_o) J_s'^2(k_{mn} r_L) \quad \text{(II.36a)}$$

$$Q_{sm} = 2\, J_{s-m}^2(k_{mn} r_o)[J_s'^2(k_{mn} r_L) + k_{mn} r_L\, J_s'(k_{mn} r_L)\, J_s''(k_{mn} r_L)] \quad \text{(II.36b)}$$

For a TE mode the coefficient K_{mn} is defined as

$$K_{mn} = (1 - \frac{m^2}{x_{mn}^2}) J_m^2(x_{mn}) \quad \text{(II.37)}$$

The TM equation becomes

$$\frac{\omega^2}{c^2} - k_{mn}^2 - k_z^2 = -\frac{2e^2\mu_o\sigma_o}{m_o r_w^2 K_{mn}} \int r_o dr_o p_t dp_t dp_z h_o(r_o) g_o(p_t, p_z)$$

$$\left\{\left[\frac{(\beta_z - \beta_{ph}^{-1})^2 (\frac{\omega\gamma}{s\Omega_e})^2}{(\omega - k_z v_z - \frac{s\Omega_e}{\gamma})^2} - \frac{1}{(\frac{s\Omega_e}{\gamma})^2}\right](\omega^2 - k_z^2 c^2)\frac{\beta_t^2}{\gamma} \tilde{H}_{sm}\right.$$

$$- \frac{(\beta_z - \beta_{ph}^{-1})^2 \frac{\omega\gamma}{s\Omega_e}}{\gamma (\omega - k_z v_z - \frac{s\Omega_e}{\gamma})\omega} \tilde{Q}_{sm}\} \qquad \text{(II.38)}$$

where

$$\tilde{H}_{sm} = [J_{s-m}(k_{mn} r_o) \frac{s}{k_{mn} r_L} J_s(k_{mn} r_L)]^2 \qquad \text{(II.39a)}$$

$$\tilde{Q}_{sm} = 2 J_{s-m}^2(k_{mn} r_o)[(\frac{s}{k_{mn} r_L})^2 J_s^2(k_{mn} r_L) + \frac{J_{s-2}(k_{mn} r_L) - J_{s+2}(k_{mn} r_L)}{4}] \qquad \text{(II.39b)}$$

For a TM mode the coefficient K_{mn} is defined as

$$K_{mn} = J_m'^2(x_{mn}) \qquad \text{(II.40)}$$

Eqs.(II.35) and (II.38) can be simplified in the case of a cold, thin annular beam. This corresponds to the delta function distribution function

$$h_o(r_o) = A_b \frac{1}{r_o} \delta(r_o - r_b) \qquad \text{(II.41a)}$$

$$g_o(p_t, p_z) = \frac{1}{2\pi p_t} \delta(p_t - p_{to}) \delta(p_z - p_{zo}) \qquad \text{(II.41b)}$$

where A_b is the area of the beam cross section and r_b is the average beam radius. It is also convenient to introduce the plasma frequency

$$\omega_p^2 = \frac{\sigma_o e^2 \mu c^2}{m_o} \qquad \text{(II.42)}$$

and the beam-waveguide fill factor

$$f_{bw} = \frac{A_b}{\pi r_w^2} \tag{II.43}$$

which is usually much less than unity. Substituting Eqs.(II.41)-(II.43) into Eqs.(II.35) and (II.38) leads to the cold beam dispersion equations for the TE mode:

$$(\omega^2 - k_{mn}^2 c^2 - k_z^2 c^2)\,(\omega - k_z v_{zo} - \frac{s\Omega_e}{\gamma_o})^2 =$$

$$- \frac{f_{bw}\omega_p^2}{K_{mn}\gamma_o}\,[(\omega^2 - k_z^2 c^2)\,\beta_{to}^2 H_{sm} - (\omega - k_z v_{zo})(\omega - k_z v_{zo} - \frac{s\Omega_e}{\gamma_o})Q_{sm}] \tag{II.44}$$

and for the TM mode:

$$(\omega^2 - k_{mn}^2 c^2 - k_z^2 c^2)\,(\omega - k_z v_{zo} - \frac{s\Omega_e}{\gamma_o})^2 =$$

$$- \frac{f_{bw}\,\omega_p^2}{K_{mn}\,\gamma_o}\,\{[(\beta_{zo} - \beta_{ph}^{-1})^2(\frac{\omega\gamma_o}{s\Omega_e})^2 - \frac{(\omega - k_z v_{zo} - \frac{s\Omega_e}{\gamma_o})^2}{(s\Omega_e/\gamma_o)^2}]\,(\omega^2 - k^2 c^2)\,\beta_{to}^2\,\bar{H}_{sm}$$

$$- (\beta_{zo} - \beta_{ph}^{-1})^2\,\frac{s\Omega_e}{\gamma_o}\,(\omega - k_z v_{zo} - \frac{s\Omega_e}{\gamma_o})\,\bar{Q}_{sm}\} \tag{II.45}$$

Eq.(II.44) agrees with the result derived previously by Chu et al (1980) except that their result includes additional terms in the expression for Q_{sm}. These terms are not included in the present analysis because the term involving $\partial f_o/\partial r_o$ in Eq.(II.20) has been neglected. In configurations optimized for the cylcotron maser interaction these terms are small. However in a related device called the peniotron which involves large electron guiding

center drifts these terms can be important (Zhang 1985). Thus the present analysis does not apply to this device. As discussed by Chu et al (1980), the first term on the RHS of Eq.(II.44) is the source of the instability, while the second is a stabilizing term. For relativistic beams with signifigant transverse velocity, the second term is much smaller than the first and can be neglected.

Comparing Eqs.(II.44) and (II.45) shows that the TE and TM mode dispersion relations are similar in form but there are significant differences. The TM mode instability tends to be reduced compared to the TE mode case by two effects: First, the RHS of Eq.(II.45) involves an additional stabilizing term proportional to $(\omega - k_z v_{zo} - s\Omega_e/\gamma)^2$. For frequencies near the doppler-shifted cyclotron frequency this term will be usuually be small compared to the others and can be neglected. Secondly, the other terms on the RHS of Eq.(II.45) include the factor $(\beta_z - \beta_{ph}^{-1})^2$ which vanishes when the beam velocity equals the wave group velocity since $v_g = c^2/v_{ph}$. Thus, the TM mode instability vanishes when the vacuum waveguide mode and beam mode are at grazing incidence. This effect has been pointed out by Abubakirov (1983).

The temporal growth rates for the instability at resonance are obtained by substituting $\omega = \omega_o + \Delta\omega$, $k_z = k_{zo}$ into the dispersion equations, where (ω_o, k_o) is the point of intersection between the uncoupled waveguide mode

$$\omega^2 - k_{mn}^2 c^2 - k_z^2 c^2 = 0 \qquad \text{(II.46)}$$

and the beam mode

$$\omega - k_z v_{zo} - s\Omega_e/\gamma_o = 0 \tag{II.47}$$

Neglecting small terms as discussed above leads to the cubic equations

$$\Delta\omega^3 = - \frac{f_{bw}\,\omega_p^2 \omega_{mn}\,\beta_{to}^2\,H_{sm}\,(1-\beta_{ph}^{-2})^{1/2}}{2\,K_{mn}\,\gamma_o} \tag{II.48}$$

and

$$\Delta\omega^3 = - \frac{f_{bw}\omega_p^2\,\omega_{mn}\,\beta_{to}^2\,\tilde{H}_{sm}\,(\beta_{zo}-\beta_{ph}^{-1})^2\,(1-\beta_{ph}^{-2})^{1/2}}{2\,K_{mn}\,\gamma_o\,(1-\beta_{zo}/\beta_{ph})^2} \tag{II.49}$$

for the the TE and TM modes, respectively. Setting $\Delta\omega = \Delta\omega_r + i\Delta\omega_i$, Eqs.(II.48) and (II.49) have the solutions

$$\Delta\omega_r = \left[\frac{f_{bw}\,\omega_p^2\,\omega_{mn}\,\beta_{to}^2\,H_{sm}\,(1-\beta_{ph}^{-2})^{1/2}}{16\,K_{mn}\gamma_o} \right]^{1/3} \tag{II.50}$$

and

$$\Delta\omega_r = \left[\frac{f_{bw}\,\omega_p^2\,\omega_{mn}\,\beta_{to}^2\,\tilde{H}_{sm}(\beta_{zo}-\beta_{ph}^{-1})^2\,(1-\beta_{ph}^{-2})^{1/2}}{16\,K_{mn}\,\gamma_o(1-\frac{\beta_{zo}}{\beta_{ph}})^2} \right]^{1/3} \tag{II.51}$$

respectively, where ω_r is the width of the beam-wave interaction. The temporal growth rate is given by

$$\Delta\omega_i = \sqrt{3}\,\Delta\omega_r \tag{II.52}$$

Inspection of Eqs.(II.50)-(II.52) shows that for a given electron beam and waveguide, the growth rate is highest for a wave near cutoff and approaches zero as the phase velocity approaches the free space value for both TE and TM modes. In addition, the growth rate vanishes at grazing incidence for TM modes ($v_z = v_g$).

As pointed out by Bratman et al (1983), this effect can be explained by considering a rest frame moving with the group velocity of the wave. In this frame the mode is at cut-off ($k_z = o$) and in the case of a TM mode has only a longitudinal electric field component. If the electron beam drift velocity $v_{zo}=v_{gr}$, then in this frame the electron motion is purely transverse and the rf field does no work on the electrons. This effect has also been pointed out by Lau (1982) for a beam with axi-centered electron orbits.

The spatial growth rate can be calculated by substituting $\omega = \omega_o$ and $k = k_o + \Delta\kappa$ into Eqs.(II.44) and (II.45). The result can be expressed as

$$\Delta k_i = \left[\frac{1}{\beta_g \beta_{zo}^2}\right]^{1/3} \frac{\Delta\omega_i}{c} \qquad \text{(II.53)}$$

where $\beta_g = \beta_{ph}^{-1}$. From Eqs.(II.50)-(II.53) the small signal spatial growth rates expressed in units of dB/m are

$$\Gamma\ (\text{dB/m}) = 7.5 \left[\frac{f_{b\omega}\ \omega_p^2\ \omega_{mn}\ \beta_{to}^2}{K_{mn}\ \gamma_o\ \beta_{zo}^2}\ J_{m-s}^2(k_{mn} r_b)\ J_s'^2(k_{mn} r_L)\right]^{1/3} (\beta_{ph}^2 - 1)^{1/6} \qquad \text{(II.54)}$$

for a TE mode, and

$$\Gamma(\mathrm{dB/m}) = 7.5\left[\frac{f_{bw}\,\omega_p^2\,\omega_{mn}\,\beta_{to}^2}{K_{mn}\,\gamma_o\,\beta_{zo}^2}\,J_{m-s}^2(k_{mn}r_b)\left(\frac{s}{k_{mn}r_L}\right)^2 J_s^2(k_{mn}r_L)\right]^{1/3}$$

$$\frac{(\beta_{ph}^{-1}-\beta_{zo})^{2/3}\,(\beta_{ph}^2-1)^{1/6}}{\left(1-\frac{\beta_{zo}}{\beta_{ph}}\right)^{2/3}} \qquad \text{(II.55)}$$

for a TM mode. Eqs.(II.54) and (II.55) do not apply when the instability becomes absolute such as occurs at the waveguide cutoff frequency. The onset of absolute instability for a TE mode at the grazing incidence condition has been analyzed by Lau et al (1981).

III. Single-Particle Theory

In this section the Cyclotron Maser interaction is treated in the single particle approximation. A thin annular beam propagating in a circular waveguide in the presence of an applied axial magnetic field is considered. The electrons follow helical trajectories in the applied magnetic field about guiding centers located at a radius r_o from the symmetry axis. Slow-time-scale nonlinear equations are obtained for the interaction with a given harmonic.

The starting point is the Lorentz force equation for an electron drifting in an applied predominantly axial magnetic field and experiencing perturbing rf fields:

$$\frac{d\vec{p}}{dt} + \frac{|e|}{\gamma}\vec{p} \times \vec{B}_o = -|e|(\vec{E} + \frac{1}{\gamma}\vec{p} \times \vec{B}) = \vec{a} \qquad \text{(III.1)}$$

where $\vec{B}_o$ is the applied magnetic field

$$\vec{B}_o = B_{oz}\hat{z} + B_{or}\hat{r} \ , \ B_{or} << B_{oz} \qquad \text{(III.2)}$$

$\vec{E}$ and $\vec{B}$ are the rf fields, and γ is the relativistic factor

$$\gamma = [1 + p^2/(m_o c)^2]^{1/2} \qquad \text{(III.3)}$$

To obtain slow-time-scale variables, the transverse momentum is expressed in the form

$$p_x + ip_y = ip_t \exp[i(\Omega\tau + \Phi)] \qquad \text{(III.4)}$$

where p_t and Φ are the slowly varying magnitude and phase, Ω is the reference cyclotron frequency

$$\Omega = \frac{|e|B_{oz}(z_o)}{\gamma_o m_o} \qquad \text{(III.5)}$$

where $z_o = z(t_o)$, and $\tau = t - t_o$ where t_o is the time the electron enters the interaction region. Substituting Eq.(III.4) into Eq.(III.1) and neglecting drifts of the electron guiding center due to the rf fields, the equations of motion can be expressed in the form

$$\frac{dp_t}{dt} = \frac{i}{2}\left[(a_x - ia_y)\, e^{i(\Omega\tau + \Phi)} - (a_x + ia_y)e^{-i(\Omega\tau + \Phi)}\right] + \frac{p_t p_z}{2m_o\gamma}\frac{1}{B_{oz}}\frac{\partial B_{oz}}{\partial z} \tag{III.6a}$$

$$\frac{d\Phi}{dt} = -\frac{1}{2}\left[(a_x - ia_y)e^{i(\Omega t+\Phi)} + (a_x + ia_y)e^{-i(\Omega\tau+\Phi)}\right]\frac{1}{p_t} - \Omega\left(1 - \frac{\gamma_o}{\gamma}\right) \tag{III.6b}$$

$$\frac{dp_z}{dt} = a_z - \frac{p_t^2}{2m_o\gamma}\frac{1}{B_{oz}}\frac{\partial B_{oz}}{\partial z} \tag{III.6c}$$

In the equations which follow the magnetic field gradient terms will be dropped corresponding to the case of a constant applied axial magnetic field. Substituting Eqs. (II.2)-(II.4), and (II.9)-(II.10) into Eqs.(III.6) leads the following equations of motion for a TE mode:

$$\frac{dp_t}{dt} = \mathrm{Re}\left\{-\frac{|e|}{2}(\Pi - v_z T)(L_+\psi e^{-i(\Omega\tau+\Phi)} + L_-\psi e^{i(\Omega\tau+\Phi)})e^{-i\omega t}\right\} \tag{III.7a}$$

$$\frac{d\Phi}{dt} = \frac{1}{2p_t}\mathrm{Re}\left\{i|e|\left[(\Pi - v_z T)(L_+\psi e^{-i(\Omega\tau+\Phi)} - L_-\psi e^{i(\Omega\tau+\Phi)}) - 2\frac{v_t k_t^2}{\omega}\Pi\psi\right] e^{-i\omega t}\right\} - \Omega\left(1 - \frac{\gamma_o}{\gamma}\right) \tag{III.7b}$$

$$\frac{dp_z}{dt} = \mathrm{Re}\left\{-\frac{|e|v_t}{2}T(L_+\psi e^{-i(\Omega\tau+\Phi)} + L_-\psi e^{i(\Omega\tau+\Phi)})e^{-i\omega t}\right\} \tag{III.7c}$$

and for a TM mode:

$$\frac{dp_t}{dt} = \frac{1}{2}\mathrm{Re}\left\{-|e|(\Pi - v_z T)(L_+\psi e^{-i(\Omega\tau+\Phi)} - L_-\psi e^{i(\Omega\tau+\Phi)})e^{-i\omega t}\right\} \tag{III.8a}$$

$$\frac{d\Phi}{dt} = \frac{1}{2p_t} \mathrm{Re}\{-|e|(\Pi - v_z T)(L_+\psi e^{-i(\Omega\tau+\Phi)} + L_-\psi e^{i(\Omega\tau+\Phi)})e^{-i\omega t}\} - \Omega(1 - \frac{\gamma_o}{\gamma}) \tag{III.8b}$$

$$\frac{dp_z}{dt} = \frac{1}{2} \mathrm{Re}\{-i|e|T[v_t(L_+\psi e^{-i(\Omega\tau+\Phi)} - L_-\psi e^{i(\Omega\tau+\Phi)}) + 2\frac{c^2k_t^2}{\omega}\psi]e^{-i\omega t}\} \tag{III.8c}$$

where

$$L_+\psi = e^{i\theta}(\frac{\partial}{\partial r} + \frac{i}{r}\frac{\partial}{\partial\theta})\psi \tag{III.9a}$$

$$L_-\psi = e^{-i\theta}(\frac{\partial}{\partial r} - \frac{i}{r}\frac{\partial}{\partial\theta})\psi \tag{III.9b}$$

By using the expression for the scalar function ψ given in Eq.(II.13) in Eqs.(III.7) and (III.8), applying Graf's Addition Theorem for Bessel functions, and considering the interaction with the sth harmonic of the cyclotron frequency, the cyclotron maser equations of motion for a circular waveguide can be written in the form:

$$\frac{dp_t}{dt} = -|e|C_{mn}J_{m-s}(k_{mn}r_o)\frac{\partial J_s(k_{mn}r_L)}{\partial r_L}\mathrm{Re}\{(\Pi - v_z T)e^{-i\Lambda}\} \tag{III.10a}$$

$$\frac{d\Lambda}{dt} = +s\frac{|e|}{p_t}C_{mn}J_{m-s}(k_{mn}r_o)\frac{s}{r_L}J_s(k_{mn}r_L)\mathrm{Re}\{i[\Pi - v_z T - \frac{k_{mn}^2 v_t^2 \gamma}{s\Omega\omega\gamma_o}\Pi]e^{-i\Lambda}\} + \omega - s\Omega\frac{\gamma_o}{\gamma} \tag{III.10b}$$

$$\frac{dp_z}{dt} = - |e| v_t C_{mn} J_{m-s}(k_{mn} r_o) \frac{\partial J_s(k_{mn} r_L)}{\partial r_L} \mathrm{Re}\{Te^{-i\Lambda}\} \qquad \text{(III.10c)}$$

for a TE mode, and

$$\frac{dp_t}{dt} = -|e| C_{mn} J_{m-s}(k_{mn} r_o) \frac{s}{r_L} J_s(k_{mn} r_L) \mathrm{Re}\{i(\Pi - v_z T)e^{-i\Lambda}\} \qquad \text{(III.11a)}$$

$$\frac{d\Lambda}{dt} = - s\frac{|e|}{p_t} C_{mn} J_{m-s}(k_{mn} r_o) \frac{\partial J_s(k_{mn} r_L)}{\partial r_L} \mathrm{Re}\{(\Pi - v_z T)e^{-i\Lambda}\} + \omega - \frac{s\Omega\gamma_o}{\gamma} \qquad \text{(III.11b)}$$

$$\frac{dp_z}{dt} = - |e| v_t \left(1 - \frac{k_{mn}^2 c^2 \gamma}{\omega s \Omega \gamma_o}\right) C_{mn} J_{m-s}(k_{mn} r_o) \frac{s}{r_L} J_s(k_{mn} r_L) \mathrm{Re}\{iTe^{-i\Lambda}\} \qquad \text{(III.11c)}$$

for a TM mode; where the phase variable has been replaced by

$$\Lambda = (\omega - s\Omega)\tau + \omega t_o - s\Phi - (m - s)\Xi_o \qquad \text{(III.12)}$$

In Eq.(III.12) Ξ_o is the polar angle of the guiding center position.

Besides the Lorentz force equations, it is useful to consider the energy equation

$$\frac{d\varepsilon}{dt} = - |e| \vec{v} \cdot \vec{E} \qquad \text{(III.13)}$$

where ε is the electron energy. Using the prescription described above, Eq.(III.13) can be written in the form

$$\frac{d\varepsilon}{dt} = -\frac{|e|v_t}{2}\,\mathrm{Re}\,\{\Pi(z)[L_+e^{-i(\Omega\tau+\Phi)}+L_-e^{i(\Omega\tau+\Phi)}]\psi e^{-i\omega t}\} \tag{III.14}$$

for a TE mode, and as

$$\frac{d\varepsilon}{dt} = \frac{|e|}{2}\,\mathrm{Re}\,\{[\frac{c^2}{\omega}v_t\frac{dT}{dz}(L_+e^{-i(\Omega\tau+\Phi)}-L_-e^{i(\Omega\tau+\Phi)}) - 2i\frac{c^2}{\omega}v_z k_t^2 T]\psi e^{-i\omega t}\} \tag{III.15}$$

for a TM mode. For a circular waveguide and a single harmonic, these equations reduce to

$$\frac{d\varepsilon}{dt} = -|e|v_t C_{mn} J'_{m-s}(k_{mn}r_o)\frac{\partial J_s(k_{mn}r_L)}{\partial r_L}\,\mathrm{Re}\,\{\Pi e^{-i\Lambda}\} \tag{III.16}$$

and

$$\frac{d\varepsilon}{dt} = |e|v_t C_{mn} J'_{m-s}(k_{mn}r_o)\frac{s}{r_L}J_s(k_{mn}r_L)\mathrm{Re}\{[\frac{c^2}{\omega}\frac{dT}{dz} + i\frac{k_{mn}^2 c^2 v_z \gamma}{\omega s\Omega\gamma_o}T]e^{-i\Lambda}\} \tag{III.17}$$

respectively.

As pointed out by Bratman et al (1981), the relationship

$$\frac{d}{dt}(\varepsilon - v_{ph}p_z) = 0 \tag{III.18}$$

holds in the case of the Cyclotron Maser interaction for a constant amplitude free space wave of the form

$$\Pi = \Pi_o e^{ik_z z} \tag{III.19}$$

where Π_o is a constant. By substituting Eq.(II.11) into (III.10c), using Eq.(III.19), and comparing with Eq.(III.16), Eq.(III.18) is readily verified for TE modes in a waveguide. Eq.(III.18) is not in general true for TM waveguide modes as can be seen by subtracting v_{ph} times Eq.(III.11c) from Eq.(III.17) to obtain:

$$\frac{d}{dt}(\varepsilon - v_{ph}p_z) = -|e|v_t C_{mn} J_{m-s}(k_{mn}r_o)\frac{s}{r_L} J_s(k_{mn}r_L) v_{ph} \frac{(1-\beta_{ph}^{-2})}{1-\frac{\beta_{zo}}{\beta_{ph}}}$$

$$\cdot \left[\frac{\Delta v_z}{v_{zo}} - \frac{\Delta\gamma}{\gamma_o} - \delta_o\right] \mathrm{Re}\{iT_o e^{-i(\Lambda - k_z z)}\} \tag{III.20}$$

where δ_o is the kinematic phase shift parameter

$$\delta_o = 1 - \frac{\beta_{zo}}{\beta_{ph}} - \frac{s\Omega}{\omega} \tag{III.21}$$

D_o is the constant wave amplitude, and $\beta_{ph} = v_{ph}/c$, $\beta_z = v_z/c$. Eq.(III.19) shows that Eq.(III.18) holds for the TM mode interaction for a constant amplitude wave only when $v_{ph} = c$, the free space limit. It is convenient to introduce the following normalized momenta and energy:

$$p_t' = p_t/(\gamma_o m_o c) \tag{III.22a}$$

$$p_z' = p_z/(\gamma_o m_o c) \tag{III.22b}$$

$$w = (\gamma_o - \gamma)/\gamma_o \tag{III.22c}$$

the normalized axial coordinate

$$Z = \omega z/c \tag{III.23}$$

and to introduce the slowly varying momentum phase

$$\theta = \Lambda - k_z z \tag{III.24}$$

Transforming to spatial derivatives, the TE mode energy and phase equations for a constant amplitude wave can then be written as:

$$\frac{dw}{dZ} = \frac{|e|}{\gamma_o m_o c\omega} \frac{p_t'}{p_z'} C_{mn} J_{m-s}(k_{mn} r_o) \frac{\partial J_s(k_{mn} r_L)}{\partial r_L} \mathrm{Re}\{\Pi_o e^{-i\theta}\} \tag{III.25a}$$

$$\frac{d\theta}{dZ} = \frac{1}{p_z'}\left[\delta_o - w(1 - \beta_{ph}^{-2})\right] + \frac{s|e|}{\gamma_o m_o c\omega} \frac{1}{p_z' p_t'}$$

$$C_{mn} J_{m-s}(k_{mn} r_o) \frac{s}{r_L} J_s(k_{mn} r_L)\left[1 - w(1 - \beta_{ph}^{-2}) - \frac{(1 - \beta_{ph}^{-2})}{(1 - \frac{\beta_{zo}}{\beta_{ph}})} p_t'^2\right] \mathrm{Re}\{i\Pi_o e^{-i\theta}\} \tag{III.25b}$$

Using conservation of energy

$$\varepsilon^2 = m_o^2 c^4 + p_t^2 c^2 + p_z^2 c^2 \tag{III.26}$$

and Eq.(III.18), the momentum amplitudes can be expressed in terms of the normalized energy as follows:

$$p_t' = \left[\beta_{to}^2 - 2\left(1 - \frac{\beta_{zo}}{\beta_{ph}}\right)w + \left(1 - \beta_{ph}^{-2}\right)w^2\right]^{1/2} \qquad \text{(III.27a)}$$

$$p_z' = \beta_{zo} - \frac{w}{\beta_{ph}} \qquad \text{(III.27b)}$$

For interactions with non-constant amplitude waves, such as occurs in a traveling wave amplifier, Eq.(III.18) does not hold for either TE or TM modes. In the case of a TE mode, a slow axial variation of the wave amplitude affects the axial momentum according to:

$$\frac{dq'}{dZ} = -\frac{|e|}{\gamma_o m_o c\omega}\frac{p_t'}{p_z'} C_{mn} J_{m-s}(k_{mn} r_o) \frac{\partial J_s(k_{mn} r_L)}{\partial r_L} \mathrm{Re}\left\{i\frac{d\Pi_o}{dZ} e^{-i\theta}\right\} \qquad \text{(III.28)}$$

where q' is defined by

$$q' = p_z' + w/\beta_{ph} \qquad \text{(III.29)}$$

For a slow variation in wave amplitude, it is sufficient to include the axial momentum correction q' in the phase equation according to:

$$\frac{d\theta}{dZ} = \frac{1}{p_z'}\left[\delta_o - w(1-\beta_{ph}^{-2}) - \frac{(q' - \beta_{zo})}{\beta_{ph}}\right] + \frac{s|e|}{\gamma_o m_o c\omega}\frac{1}{p_t' p_z'} C_{mn} J_{m-s}(k_{mn} r_o)$$

$$\frac{s}{r_L} J_s(k_{mn} r_L)\left\{\left[1 - \frac{\beta_{zo}}{\beta_{ph}} - w(1 - \beta_{ph}^{-2}) - \frac{(1 - \beta_{ph}^{-2})}{(1 - \frac{\beta_{zo}}{\beta_{ph}})} p_t'^2\right]\mathrm{Re}\{i\Pi_o e^{-i\theta}\}\right.$$

$$\left. - (q' - \frac{w}{\beta_{ph}})\ \mathrm{Re}\left\{\frac{dT_o}{dZ} e^{-i\theta}\right\}\right\} \qquad \text{(III.30)}$$

A similar analysis leads to somewhat more complicated equations for the TM mode interaction:

$$\frac{dw}{dZ} = \frac{|e|}{\gamma_o m_o \omega} \frac{p_t'}{p_z'} C_{mn} J_{m-s}(k_{mn} r_o) \frac{s}{r_L} J_s(k_{mn} r_L)$$

$$\left[\left[\frac{\beta_{ph}^{-1} - q' + \frac{1}{\beta_{ph}}(1 - \beta_{ph}^{-2}) + \frac{1}{\beta_{ph}^2}(q' - \beta_{zo})}{1 - \beta_{zo}/\beta_{ph}}\right] \mathrm{Re}\{iT_o e^{-i\theta}\} + \mathrm{Re}\left\{\frac{dT_o}{dZ} e^{-i\theta}\right\}\right]$$

(III.31a)

$$\frac{d\theta}{dZ} = \frac{1}{p_z'}\left[\delta_o - w(1-\beta_{ph}^{-2}) - (q' - \beta_{zo})/\beta_{ph}\right] - \frac{s|e|}{\gamma_o m_o \omega} \frac{1}{p_t' p_z'} C_{mn} J_{m-s}(k_{mn} r_o) \frac{\partial J_s(k_{mn} r_L)}{\partial r_L}$$

$$\left[(\beta_{ph}^{-1} - q')\ \mathrm{Re}\{T_o e^{-i\theta}\} - \mathrm{Re}\left\{i \frac{dT_o}{dZ} e^{-i\theta}\right\}\right] \qquad \text{(III.31b)}$$

$$\frac{dp_z}{dZ} = -\frac{|e|}{\gamma_o m_o \omega} \frac{p_t'}{p_z'} C_{mn} J_{m-s}(k_{mn} r_o) \frac{s}{r_L} J_s(k_{mn} r_L)\left[\frac{1}{\beta_{ph}(1 - \frac{\beta_{zo}}{\beta_{ph}})} \frac{\beta_{ph}^{-1} - \beta_{zo}}{} + \frac{(1-\beta_{ph}^{-2})}{1 - \frac{\beta_{zo}}{\beta_{ph}}} w\right]$$

$$\mathrm{Re}\{iT_o e^{-i\theta}\} \qquad \text{(III.31c)}$$

$$\frac{dp_t'}{dZ} = -\frac{|e|}{\gamma_o m_o \omega} \frac{C_{mn}}{p_z'} J_{m-s}(k_{mn} r_o) \frac{s}{r_L} J_s(k_{mn} r_L)\left[(\beta_{ph}^{-1} - q')\mathrm{Re}\{iT_o e^{-i\theta}\} + \mathrm{Re}\left\{\frac{dT_o}{dZ} e^{-i\theta}\right\}\right]$$

(III.31d)

In the CARM regime (Bratman et al 1981) the phase velocity is close to the speed of light and the following conditions apply:

$$1 - \beta_{ph}^{-2} << 1 \qquad \text{(III.32a)}$$

$$1 - \beta_{ph}^{-2} << 1 - \frac{\beta_{zo}}{\beta_{ph}} \tag{III.32b}$$

Under these conditions Eq.(III.18) holds to a good approximation for TM modes so that that momentum amplitudes can be calculated from Eqs.(III.27). Using this fact and neglecting terms proportional to $(1 - \beta_{ph}^{-2})/(1 - \beta_z/\beta_{ph})$, the equations of motion for the CARM regime become

$$\frac{dw}{dZ} = \frac{|e|}{\gamma_o m_o c\omega} \frac{p_t'}{p_z'} C_{mn} J_{m-s}(k_{mn} r_o) \frac{\partial J_s(k_{mn} r_L)}{\partial r_L} \mathrm{Re}\{\Pi_o e^{-i\theta}\} \tag{III.33a}$$

$$\frac{d\theta}{dZ} = \frac{1}{p_z'} \left[\delta_o - w(1 - \beta_{ph}^{-2}) - \frac{q' - \beta_{zo}}{\beta_{ph}}\right] + \frac{s|e|}{\gamma_o m_o c\omega} (1 - \frac{\beta_{zo}}{\beta_{ph}}) \frac{1}{p_z' p_t'} C_{mn} J_{m-s}(k_{mn} r_o) \frac{s}{r_L} J_s(k_{mn} r_L) \mathrm{Re}\{i\Pi_o e^{-i\theta}\} \tag{III.33b}$$

for a TE mode and

$$\frac{dw}{dZ} = \frac{|e|}{\gamma_o m_o \omega} \frac{p_t'}{p_z'} \frac{(\beta_{ph}^{-1} - \beta_{zo})}{1 - \frac{\beta_{zo}}{\beta_{ph}}} C_{mn} J_{m-s}(k_{mn} r_o) \frac{s}{r_L} J_s(k_{mn} r_L) \mathrm{Re}\{iT_o e^{-i\theta}\} \tag{III.34a}$$

$$\frac{d\theta}{dZ} = \frac{1}{p_z'} \left[\delta_o - w(1 - \beta_{ph}^{-2}) - \frac{q' - \beta_{zo}}{\beta_{ph}}\right] - \frac{s|e|}{\gamma_o m_o \omega} (\beta_{ph}^{-1} - \beta_{zo}) \frac{1}{p_z' p_t'} C_{mn} J_{m-s}(k_{mn} r_o) \frac{\partial J_s(k_{mn} r_L)}{\partial r_L} \mathrm{Re}\{T_o e^{-i\theta}\} \tag{III.34b}$$

$$\frac{dq'}{dZ} = \frac{|e|}{\gamma_o m_o \omega} \frac{p_t'}{p_z'} C_{mn} J_{m-s}(k_{mn} r_o) \frac{s}{r_L} J_s(k_{mn} r_L) \mathrm{Re}\{\frac{dT_o}{dZ} e^{-i\theta}\} \qquad \text{(III.34c)}$$

for a TM mode, where the effect of non-constant wave amplitude is neglected except in the phase equation. In Eq.(III.33b), q' is given by Eq.(III.28). To further simplify the equations, the following variables defined by Bratman et al (1981) are introduced:

$$u = \frac{2}{\beta_{to}^2} (1 - \frac{\beta_{zo}}{\beta_{ph}}) w \qquad \text{(III.35a)}$$

$$\Delta = \frac{2(1 - \frac{\beta_{zo}}{\beta_{ph}})}{\beta_{to}^2 (1 - \beta_{ph}^{-2})} \delta_o \qquad \text{(III.35b)}$$

$$b = \frac{\beta_{to}^2}{2\beta_{zo}\beta_{ph}(1 - \beta_{zo}/\beta_{ph})} \qquad \text{(III.35c)}$$

$$\zeta = \frac{\beta_{to}^2}{2\beta_{zo}} \frac{(1 - \beta_{ph}^{-2})}{(1 - \frac{\beta_{zo}}{\beta_{ph}})} Z \qquad \text{(III.35d)}$$

$$\hat{q} = \frac{4\beta_{zo}}{\beta_{to}^4} \frac{(1 - \frac{\beta_{zo}}{\beta_{ph}})^2}{(1 - \beta_{ph}^{-2})} (q' - \beta_{zo}) \qquad \text{(III.35e)}$$

In this notation the momentum amplitudes in the CARM regime are given by:

$$p_t' = \beta_{to}\sqrt{1 - u} \qquad \text{(III.36a)}$$

$$p_z' = \beta_{zo}(1 - bu) \qquad \text{(III.36b)}$$

The parameter b characterizes how strongly the axial momentum and velocity change with change in electron energy.

In Cyclotron Maser interactions with the fundamental or low order harmonics the electron Larmor radius is usually small compared to the transverse dimensions of the waveguide mode. In this case the Bessel function of order s - 1 occurring in the equations of motion may be replaced by the leading term of the small argument expansion with little loss of accuracy. In terms of the present notation

$$J_{s-1}(k_{mn}r_L) = \frac{S^{s-1}(1 - \beta_{ph}^{-2})^{\frac{s-1}{2}} \beta_{to}^{s-1} \sqrt{1 - u}^{s-1}}{2^{s-1}(S-1)!\left(1-\frac{\beta_{zo}}{\beta_{ph}}\right)^{s-1}} \qquad \text{(III.37)}$$

The wave amplitudes are normalized according to:

$$F_s(TE) = \frac{4|e|}{\gamma_o m_o c^2} \frac{(1 - \frac{\beta_{zo}}{\beta_{ph}})^2 C_{mn} J_{m-s}(k_{mn}r_o)\, s^s}{\beta_{to}^3(1-\beta_{ph}^{-2})^{1/2}\, 2^s s!} \left\{ \frac{\sqrt{1 - \beta_{ph}^{-2}}}{(1 - \frac{\beta_{zo}}{\beta_{ph}})} \beta_{to} \right\}^{s-1} \Pi$$

(III.38)

for a TE mode and

$$F_s(TM) = \frac{4|e|}{\gamma_o m_o c} \frac{(\beta_{ph}^{-1} - \beta_{zo})(1 - \frac{\beta_{zo}}{\beta_{ph}})}{\beta_{to}^3 (1 - \beta_{ph}^{-2})^{1/2}} C_{mn} J_{m-s}(k_{mn} r_o) \frac{s^s}{2^s s!} \left\{ \frac{\sqrt{1 - \beta_{ph}^{-2}}}{(1 - \frac{\beta_{zo}}{\beta_{ph}})} \beta_{to} \right\}^{s-1} T \tag{III.39}$$

for a TM mode. Using Eqs.(III.35) - (III.39), the CARM energy and phase equations of motion may be reduced to the following form:

$$\frac{du}{d\zeta} = \frac{[1 - u]^{s/2}}{1 - bu} \mathrm{Re}\{F_s e^{-i\theta}\} \tag{III.40a}$$

$$\frac{d\theta}{d\zeta} = \frac{1}{(1-bu)} \left[\Delta - u - b\hat{q} + \frac{s}{2}(1 - u)^{\frac{s}{2} - 1} \mathrm{Re}\{iF_s e^{-i\theta}\}\right] \tag{III.40b}$$

for TE modes, and to

$$\frac{du}{d\zeta} = \frac{[1-u]^{s/2}}{1-bu} \mathrm{Re}\{iF_s e^{-i\theta}\} \tag{III.41a}$$

$$\frac{d\theta}{d\zeta} = \frac{1}{1-bu} \left[\Delta - u - b\hat{q} - \frac{s}{2}(1-u)^{\frac{s}{2} - 1} \mathrm{Re}\{F_s e^{-i\theta}\}\right] \tag{III.41b}$$

for TM modes. For non-constant wave amplitudes, the axial momentum correction is given by

$$\frac{d\hat{q}}{d\zeta} = - \frac{[1-u]^{s/2}}{1-bu} \mathrm{Re}\left\{i \frac{dF_s}{d\zeta} e^{-i\theta}\right\} \tag{III.42}$$

for TE modes and by

$$\frac{d\hat{q}}{d\zeta} = \frac{(1 - \frac{\beta_{zo}}{\beta_{ph}})}{(\beta_{ph}^{-1} - \beta_{zo})} \frac{[1-u]^{s/2}}{(1-bu)} \mathrm{Re}\{\frac{dF_s}{d\zeta} e^{-i\theta}\} \qquad \text{(III.43)}$$

for TM modes.

The above equations describe the motion of an electron subject to prescribed rf fields. In a self-consistent formulation the wave amplitudes should be calculated from the induced AC current and charge densities. Assuming a time dependence of the form $\exp(-i\omega t)$, the following wave equations are obtained from Maxwell's Equations appropriate for TE and TM modes, respectively:

$$(\nabla^2 + (\frac{\omega}{c})^2) \vec{E}_t = - i\mu_o \omega \vec{J}_{t\omega} \qquad \text{(III.44a)}$$

$$(\nabla^2 + (\frac{\omega}{c})^2) E_z = -i\mu_o \omega J_{z\omega} + \frac{1}{\epsilon_o} \nabla_z \rho_\omega \qquad \text{(III.44b)}$$

where in Eqs.(III.44) $\vec{E}$ and E_z are complex phasors and $\vec{J}_{t\omega}$, $J_{z\omega}$, and ρ_ω are the fundamental Fourier components of the AC current and charge densities. Using the prescription outlined by Flyagin et al (1977) and by Fliflet et al (1982), the following wave equations for the z-dependent mode amplitudes Π and T can be derived:

$$(\nabla_z^2 + k_z^2) \Pi = 2i\mu_o I_o \omega C_{mn} J_{m-s}(k_{mn} r_o) \frac{1}{2\pi} \int_o^{2\pi} d\Lambda_o \frac{p_t'}{p_z'} \frac{\partial J_s(k_{mn} r_L)}{\partial r_L} e^{i\Lambda} \qquad \text{(III.45a)}$$

$$(\nabla_z^2+k_z^2)T = \frac{2\mu_o I_o \omega}{c} \frac{(\beta_{ph}^{-1}-\beta_{zo})}{(1-\frac{\beta_{zo}}{\beta_{ph}})} C_{mn} J_{m-s}(k_{mn}r_o) \frac{1}{2\pi}\int_o^{2\pi} d\Lambda_o \frac{p_t'}{p_z'} \frac{s}{r_L} J_s(k_{mn}r_L) e^{i\Lambda} \tag{III.45b}$$

where the Eq.(45a) applies to TE modes and Eq.(III.45b) applies to TM modes. Considering the interaction with a co-propagating wave, i.e., $\Pi = \Pi_o \exp(ik_z z)$, $T = T_o \exp(ik_z z)$, neglecting second derivatives of Π_o or T_o, introducing normalized variables, and approximating the Bessel functions of order s, leads to the following equations for the normalized TE wave amplitude:

$$\frac{dF_s}{d\zeta} = \hat{I}_{TE} \frac{1}{2\pi}\int_o^{2\pi} d\theta_o \frac{\sqrt{1-u}^s}{1-bu} e^{i\theta} \tag{III.46}$$

and for the TM wave amplitude:

$$\frac{dF_s}{d\zeta} = -i\,\hat{I}_{TM} \frac{1}{2\pi}\int_o^{2\pi} d\theta_o \frac{\sqrt{1-u}^s}{1-bu} e^{i\theta} \tag{III.47}$$

where the normalized current parameter is given by:

$$\hat{I}_{TE} = \frac{8\mu_o |e| I_o \beta_{ph}}{m_o c \gamma_o \beta_{to}^4} C_{mn}^2 J_{m-s}^2(k_{mn}r_o) \frac{(1-\frac{\beta_{zo}}{\beta_{ph}})^3}{(1-\beta_{ph}^{-2})} \left\{\frac{s^s}{2^s s!}\left[\frac{\sqrt{1-\beta_{ph}^{-2}}}{(1-\frac{\beta_{zo}}{\beta_{ph}})}\beta_{to}\right]^{s-1}\right\}^2 \tag{III.48}$$

for a TE mode and by:

$$\hat{I}_{TM} = \frac{(\beta_{ph}^{-1}-\beta_{zo})^2}{(1-\frac{\beta_{zo}}{\beta_{ph}})^2} \hat{I}_{TE} \tag{III.49}$$

for a TM mode. Eqs.(III.40), (III.42) and (III.46) form a self-consistent set for the TE mode traveling wave interaction. Similarly, Eqs.(III.41), (III.43) and (III.47) form a self-consistent set for the TM mode traveling wave interaction in the CARM regime. Although the derivation has been carried out for the CARM regime, it is readily shown that the above equations apply in the gyrotron limit as well ($b \to o$, $\beta_{ph} \to \infty$).

It is of interest to compare the results of single particle theory with the results of the kinetic theory derived above for a tenuous beam with δ - function distributions. Expressing the wave amplitude in the form

$$F_s = F_{so} e^{-i(\Gamma - \Delta)\zeta}, \tag{III.50}$$

solving the single particle equations in the small signal limit and averaging with respect to the initial electron phase leads to:

$$(\Gamma - \Delta)\left(\Gamma^2 + \frac{b\hat{I}}{2}\right) - \frac{s\Gamma\hat{I}}{2} + \frac{\hat{I}}{2} = 0 \tag{III.51}$$

for a TE mode, and

$$(\Gamma - \Delta)\left[\Gamma + \frac{b(1-\kappa)\hat{I}}{2} - \frac{s\Gamma\hat{I}}{2}\right] + \frac{\hat{I}}{2} = 0 \tag{III.52}$$

for a TM mode where

$$\kappa = \frac{\left(1 - \frac{\beta_{zo}}{\beta_{ph}}\right)}{\beta_{ph}^{-1} - \beta_{zo}} \tag{III.53}$$

When the beam current parameter is small, Eqs.(III.51) and (III.52) reduce to

$$(\Gamma - \Delta)\,\Gamma^2 = -\frac{\hat{I}}{2} \tag{III.54}$$

which - as pointed out by Bratman et al (1981) - has the same form as the well-known Traveling-Wave Tube amplifier dispersion equation (Gewartowski and Watson, 1965). The normalized growth rate at resonance ($\Delta = 0$) is then given by

$$\mathrm{Im}\Gamma = \frac{\sqrt{3}}{2}\left[\frac{\hat{I}}{2}\right]^{1/3} \tag{III.55}$$

for either TE or TM modes.

By substituting unnormalized parameters into Eqs.(III.55) and (III.62) and using the small argument approximation for the appropriate Bessel functions in Eqs.(II.50) - (II.51), it is readily shown that the single particle TE and TM mode growth rates agree with the kinetic theory results given in Eqs.(II.50) - (II.53).

In terms of the present normalized parameters, the electronic efficiency is given by:

$$\eta = \frac{\beta_{to}^2 \langle u(\mu)\rangle}{2\left(1 - \frac{\beta_{zo}}{\beta_{ph}}\right)\left(1 - \gamma_o^{-1}\right)} \tag{III.56}$$

where μ is the point where the interaction terminates and $\langle\ \rangle$ denotes averaging with respect to the initial momentum phase angle. The total time-averaged power of a traveling-wave integrated over the waveguide cross section at any point is given by:

$$P_\omega = \frac{k_z}{2\mu_o\omega}|\Pi_o|^2 \tag{III.57}$$

In a high Q oscillator, the RF field axial profile is essentially determined by the cavity and not by the interaction with the beam. In this case the equation for the field amplitude can be neglected and the efficiency can be found by integrating the equations of motion in a prescribed cavity RF field. The required beam power is found by applying the power balance equation

$$\eta I_o V_o = \frac{\omega W}{Q} \tag{III.58}$$

where V_o is the beam voltage, Q is the cavity Q factor neglecting wall losses, and W is the cavity stored energy which is given by

$$W = \frac{1}{2}\,\varepsilon_o \int_{z_{in}}^{z_{out}} dz|\Pi(z)|^2 = \frac{1}{2}\,\frac{1}{\mu_o} \int_{z_{in}}^{z_{out}} dz|T(z)|^2 \tag{III.59}$$

For a cavity defined by a uniform waveguide terminated by sections of high reflectivity, the field amplitude is uniform and the stored energy is given by:

$$W = \frac{1}{2}\,\varepsilon_o L|\Pi_o|^2 \tag{III.60}$$

The small signal efficiency for a uniform field amplitude and the s^{th} harmonic is given by:

$$\eta_s^{(ss)} = \frac{\beta_{to}^2 F_s^2 \mu^2 [-(s-b)\phi - (1-b\Delta)\mu\phi']}{4(1 - \frac{\beta_{zo}}{\beta_{ph}})(1 - \gamma_o^{-1})} \qquad \text{(III.61)}$$

where

$$\phi = \frac{1 - \cos \Phi_K}{\Phi_K^2} , \qquad \text{(III.62a)}$$

$$\phi' = \frac{d\phi}{d\Phi_K} = \frac{\sin\Phi_K}{\Phi_K^2} - \frac{2\phi}{\Phi_k} , \qquad \text{(III.62b)}$$

$$\Phi_K = \Delta\mu , \qquad \text{(III.62c)}$$

$$\mu = \frac{\beta_{to}^2 (1 - \beta_{ph}^{-2})}{2\beta_{zo}(1 - \frac{\beta_{zo}}{\beta_{ph}})} \frac{\omega L}{c} , \qquad \text{(III.62d)}$$

and L is the interaction length. The parameter Φ_K corresponds to the parameter Δ defined by Chu (1978). Considering the small signal limit, substituting Eq.(III.61) into Eq.(III.58), and transforming to normalized variables leads to the following expression for the threshold beam current for either TE or TM modes:

$$\hat{I}_{thr} = \frac{2\beta_{zo}\beta_{ph}(1 - \frac{\beta_{zo}}{\beta_{ph}})}{Q\beta_{to}^2\mu(1 - \beta_{ph}^{-2})[-(s-b)\phi - (1-b\Delta)\mu\phi']} \qquad \text{(III.63)}$$

The Q factor for a cavity with uniform wave amplitude is given by

$$Q = 2\beta_{ph} \frac{\omega L}{c} \frac{1}{(1 - R_1 R_2)} \qquad \text{(III.64)}$$

where R_1 and R_2 are the reflection coefficients at the cavity input and output. Substituting Eq.(III.64) into (III.63) leads to

$$\hat{I}_{thr} = \frac{1 - R_1 R_2}{2\mu^2[-(s-b)\phi - (1 - b\Delta)\mu\phi']} \qquad \text{(III.65)}$$

IV. CALCULATIONS

A. High Q oscillator

Applications of the present theory have been considered by several authors, therefore only selected calculations are presented here.

In the case of a high-Q oscillator with a uniform axial magnetic field, the electrons interact with an approximately constant amplitude wave and the normalized efficiency $\hat{\eta} = \langle u \rangle$ depends on only five parameters: the wave amplitude F_o, the interaction length μ, the detuning parameter Δ, the harmonic number s, and the parameter b which characterizes how strongly the electron longitudinal velocity changes with a change in electron energy during the interaction. A theory of the quasi-optical gyrotron which corresponds to $b = 0$, involving four parameters was obtained by Bondeson, Manheimer and Ott (1983). In the following calculations the detuning parameter is treated as an optimization variable. Figure 2 shows the normalized efficiency $\hat{\eta}$ as a function of b for several values of F_o. The calculations are for s=1 and are optimized with respect to μ. The corresponding values of μ are given in

Figure 3. Figure 4 compares efficiency of the first four harmonics for F_o = 0.2 and optimized Δ and μ. The optimum interaction lengths for the higher order harmonics (not shown) are only slightly different from the results for s=1. The actual efficiency is obtained for these results by using Eq. (III.56). Note that the results given in Figures 2 and 3 are independent of mode, electron energy and orbit pitch angle, and the wave frequency and phase velocity.

The limit b = 0 corresponds to the gyrotron interaction where the wave is close to cutoff and the wave frequency is approximately equal to the relativisitc cyclotron frequency. This limit gives the highest normalized efficiency ($\hat{\eta}$ = 42%) and has been extensively investigated. As is well known the efficiency for this limit can be enhanced considerably by contouring the axial profile of the RF field. Normalized efficiencies of order 80% have been reported (Gaponov et al 1981).

As discussed by Bratman et al (1981,1983), the Cyclotron Auto-Resonance Maser (CARM) regime corresponds to b = 0.5. The single-particle efficiency is optimized ($\eta_{sp} \lesssim 0.5$) by choosing $\beta_t = 1/\gamma$. A large doppler upshift - $\omega \lesssim \gamma^2\Omega_c$ where Ω_c is the relativistic cyclotron frequency - and good bunching efficiency (characterized by $\hat{\eta}$) occur when in addition $(1-\beta_{ph}^{-2}) < \gamma^{-2}$. Figure 2 shows that a maximum normalized efficiency of 36% is obtained at b = 0.5 for F_o = 0.2, Δ = 0.6, and μ = 8. This result was given previously by Bratman et al (1981). One expects that considerably higher efficiencies should be achievable by enhancement techniques similar to those used in gyrotrons.

Another regime of doppler-shifted operation has been investigated by Vomvoridis (1982) for the oscillator and by Ginzburg, Zarnitsyna, and Nusinovich (1981). In this case $\beta_{zo} = (1-\gamma_o^{-1})/\beta_{ph}$ and $\beta_{to}^2 = 2\beta_{ph}^{-2}\gamma_o^{-1}(1-\gamma_o^{-1}) + (1-\beta_{ph}^{-2})(1-\gamma_o^{-2})$. An interesting feature of this choice is both β_t and β_z can vanish simultaneously, that is, the total kinetic energy is available to the interaction (Vomvoridis 1982) and the single-particle efficiency approaches 100%. In this regime $b = 1$ and, as shown in Figure 2, the maximum normalized (and unnormalized) efficiency is 22%. As in the other regimes, higher efficiencies should be achievable through enhancement techniques.

Based on these calculations design parameters are given in Table I for a 100 GHz CARM oscillator experiment using 600 kV beam and choosing $\beta_{to} = 1/\gamma_o$.

B. Traveling-Wave Amplifier

Calculations have been carried out to investigate a CARM regime amplifier. Figure 5a shows the normalized efficiency as a function of normalized current for $b = 0.454$ and $F_o = 0.0018$. The results have been optimized with respect to Δ and interaction length μ. As pointed out by Ginzburg, Zarnitsyna and Nusinovich (1981) the saturated efficiency and wave amplitude are independent of the input amplitude when the input amplitude is sufficiently small. The results shown in Figure 5 represent this limit. The values of saturation wave amplitude and interaction length corresponding to Figure 5a are shown in Figures 5b and 5c, respectively. Except at low beam current ($\hat{I}_o < 0.05$) which requires smaller values, the optimum detuning is $\Delta = 0.4$.

The effect of increasing the input wave amplitude for a given beam current is shown in Figure 6 for a normalized current of $\hat{I}_o = 0.60$ and $b = 0.47$. The results have been optimized with respect to Δ and μ as in Figure 5. Figure 6a gives the normalized efficiency dependence on the input wave amplitude. As noted above, the efficiency is essentially constant over a wide range of input amplitude, then rises and saturates at a power gain of about 10 dB. The values of saturation wave amplitude and interaction length are shown in Figures 6b and 6c. The optimum detuning is $\Delta \approx 0.4$.

The design of a high power CARM amplifier operating in the TE_{11} circular waveguide mode with parameters similar to the NRL VEBA free electron laser experiment (Gold et al 1984) has been considered. The design parameters are given in Table II. The beam energy is 1 MeV, the current is 500 Amps, the waveguide radius is 5.4 mm, and the design operating frequency is 94 GHz. Figure 7 compares the small signal spatial growth rates for the TE_{11} and TM_{01} modes as a function of wave phase velocity (and frequency) in the design waveguide ($r_w = 0.54$). The growth rates were calculated using the parameters of Table II and Eqs.(II.54) and (II.55) with small argument expansions for the Bessel functions with argument $k_{mn}r_L$. The guiding center radius was taken to be zero for the TE_{11} mode and as 2.1 mm for the TM_{01} mode. Figure 7 shows as discussed above that the TM_{01} growth rate vanishes at the grazing incidence condition ($\beta_{ph}^{-1} = \beta_{zo} = 0.88$). Except for this effect for TM modes, the growth rates increase monotonically as the wave approaches the cut-off condition. This calculation assumes the instability is convective, at some point it becomes absolute and the calculation is invalid (see Lau et al 1981).

The peak output power of the design is 110 MW at an electronic efficiency of 22% ($\langle u \rangle = 0.34$). The normalized interaction length is $\mu = 15.4$ for an input power of 1 kW ($F_o = 0.0019$) and the total gain is 50 dB. The small signal and nonlinear efficiencies are plotted as a function of the detuning parameter Δ in Figure 8. The small signal result has been scaled by a factor of 10 for clarity. Both curves were calculated numerically, the small signal results correspond to an input power of 1 W and the nonlinear results correspond to 1 kW. The FWHM linear and nonlinear bandwidths are 10% and 3%, respectively. Note that the bandwidth cannot be directly obtained from Figure 8 because Δ is not proportional to frequency. The bandwidth could be increased by decreasing the total gain. Figure 8 shows that the region of maximum nonlinear gain is signifigantly detuned from the region of maximum small signal gain.

As a final example a 2 THz second harmonic (s=2) CARM amplifier is considered. Operation at high power at this frequency requires that the waveguide transverse dimension be much larger than the radiation wavelength (λ=0.15 mm). This can be achieved partly by operating in a higher order mode but primarily by locating the beam line - waveguide mode intersection point far above the waveguide cut-off. This case represents the "auto-resonance" limit, however, as discussed above the rate of gain is reduced leading to a longer interaction length and increased sensitivity to beam velocity spread. In addition, there is an increased probability for exciting spurious modes. Nevertheless, this design regime is of interest due to the lack of high power sources at THz frequencies.

The waveguide radius is chosen to be 0.5 cm which allows an annular electron beam of radius 0.4 cm, and the operating mode is chosen to be the $TE_{10,1}$ whispering gallery mode. This corresponds to a wave frequency to cut-off frequency ratio of ω/ω_{co}= 17.8 or a wave phase velocity of 1.0016c. For a 1.2 MeV beam interacting at the second harmonic and with $\beta_{to}= \gamma_o^{-1}$ the doppler upshift factor is $\omega/s\Omega$ = 10.2. The required magnetic field is 115 kG which is within the state-of-the-art for superconducting solenoids. The design was optimized for a beam current of 1 kA and assumes an input power of 1 kW. The maximum efficiency and power were calculated to be 19% and 223 MW at an interaction length of 134 cm. The nonlinear instantaneous bandwidth is approximately 0.04% and the total gain is 53 dB corresponding to an average gain rate of 0.4 dB/cm. The design parameters are summarized in Table III. The normalized parameters for this design are b=0.518, $\hat{I}_o$=0.0044, F_o=0.0001, F_{sat}=0.050, μ=92, Δ=0.15, and $\langle u \rangle$=0.28.

V. Conclusions

A comprehensive theory of the Cyclotron Resonance Maser interaction in a waveguide has been presented, including the kinetic theory and single particle theory approaches. The interaction has been examined for both TE and TM modes, and equations have been expressed in a simple form which elucidates the physics and facilitates calculation. The kinetic theory was used to derive dispersion relationships for generalized beam parameters and to calculate growth rates for a cold beam. The single particle theory was used to obtain linear and nonlinear results for a cold beam. The present results confirm that the form of the equations of motion and the dispersion relationships is the same for TE and TM modes in the CARM and gyrotron regimes. The theory

provides the starting point for treating electron beam self-field effects, the use of plasma filled waveguides, and the treatment of time dependent phenomenea.

The calculations carried out for the oscillator configuration as a function of the parameter b apply to essentially all possible CRM configurations including gyrotrons (b = 0), CARM's (b = 0.5), and highly relativistic doppler shifted configurations with high pitch angle beams (b = 1). Comparison of the latter two regimes shows that normalized efficiency is higher at b = 0.5 than at b = 1, but the single particle efficiency is higher at b = 1 ($\eta_{sp} \leq 100\%$) than at b = 0.5 ($\eta_{sp} \leq 50\%$) . Thus the actual efficiency is similar in the two cases (20-25%).

These calculations show that the doppler-shifted cyclotron maser interaction is an attractive candidate for use in high power, high frequency sources. Nonlinear efficiencies of order 25% are feasible and this can be increased by enhancement techniques. The CARM regime appears to offer an attractive combination high interaction efficiency, large doppler upshift, and low beam orbit pitch angle. Examples of amplifier and oscillator configurations are given. These examples show the potential of the CARM configuration as a high power millimeter-wave and sub-millimeter-wave source operating at the 50-200 MW level. The present calculations do not account for beam temperature or velocity spread. CARM amplifier simulation studies by Lin and Lin (1985) indicate that less than 1% axial velocity spread is required to achieve high efficiency in a configuration similar to the present 94 GHz example. The shorter interaction length of the CARM oscillator should render it less sensitive to velocity spread: the calculations of Kanavets and Klimov

(1975) suggest the transverse velocity spread (standard deviation) should be less than 5%.

VI. Acknowledgements

Many helpful discussions with Drs. W. M. Manheimer, S. H. Gold, V. L. Granatstein, K. R. Chu and A. K. Ganguly are gratefully acknowledged. This work was supported by the Office of Naval Research.

REFERENCES

Abramowitz, M., and Stegun, I.A., 1964, Handbook of Mathematical Functions Washington GPO p. 355

Abubakirov, E. B., 1983, Excitation of transverse magnetic waves and mode selection in relativistic cyclotron-resonance masers. Izv. Vssh. Ucheb. Zaved. Radiofizika, 26, 492-496 [Radiophysics and Quantum Electronics, 26, 379-383].

Bondeson, A., Manheimer, W. M., and Ott, E., 1983, Multimode analysis of quasi-optical gyrotrons and gyroklystrons. Infrared and Millimeter Waves, 9, (Edited by K.J. Button, Academic Press), Chapter 7.

Bratman, V. L., Denisov, G. G., Ginzburg, N. S., Petelin, M. I., 1983, FEL's with Bragg reflection resonators: cyclotron autoresonance masers versus ubitrons. IEEE J. Quantum Electronics, QE-19, 282-296.

Bratman, V. L., Ginzburg, N. S., Nusinovich, G. S., Petelin, M. I., and Strelkov, P.S., 1981, Relativistic gyrotrons and cyclotron autoresonance masers. Int. J. Elect., 51, 541-567.

Chu, K. R., 1978, Theory of electron cyclotron maser interaction in a cavity at the harmonic frequencies. Phys. Fluids, 21, 2354-2364.

Chu, K. R., and Dialetis, D., 1985, Kinetic theory of Harmonic Gyrotron oscillator with slotted resonant structure. Infrared and Millimeter Waves, 13, (Edit. by K. J. Butt n, Academic Press), Chapter 3.

Chu, K. R., Drobot, A. T., Szu, H. H., and Sprangle, P., 1980, Theory and simulation of the gyrotron traveling wave amplifier operating at cyclotron harmonics. IEEE Trans. Microwave Theory and Techniques, MTT-28, 313-317.

Dohler, G., Gallager, D., and Moats, R., 1978, The peniotron: a fast-wave device for efficient high power mm-wave generation. International Electron Devices Meeting Tech. Digest, 400-403.

Fliflet, A. W., Read, M. E., Chu, K. R., and Seeley, R., 1982, A self-consistent field theory for gyrotron oscillators: application to a low Q gyromonotron. Int. J. Electronics, 53, 505-521.

Flyagin, V. A., Gaponov, A. V., Petelin, M. I., and Yulpatov, V. K., 1977, The gyrotron. IEEE Trans. on Microwave Theory and Techniques, MTT-25, 514-521.

Gapanov, A. V., Petelin, M. I., and Yulpatov, V. K., 1967, The induced radiation of excited classical oscillators and its use in high-frequency electronics. Izvestia VUZ. Radiofizika, 10, 1414-1453 [Radiophysics and Quantum Electronics, 10, 794-813].

Gewartowski, J. W., and Watson, H. A., 1965, Principles of Electron Tubes (Van Nostrand), Chapter 10.

Ginzburg, N. S., Zarnitsyna, I. G., and Nusinovich, G. S., 1981, Theory of relativistic cylotron-resonance maser amplifiers. Izv. Vssh. Ucheb. Zaved., Radiofizika, 24, 481-490. [Radiophysics and Quantum Electronics, 24, 331-338].

Gold, S. H., Hardesty, D. L., Kinkead, A. K., Barnett, L. R., and Granatstein, V. L., 1984, A high-gain 35 GHz free-electron laser amplifier experiment. Phys. Rev. Lett., 52, 1218-1221.

Kanavets, V. I. and Klimov, O. I., 1976, The electron efficiency of a monotron and klystron with a relativistic polyhelical electron beam. Radiotekhnika i Electronika, 21, 2359-2364 [Radio Engng Electron Phys., 21, No. 11, 78-83].

Krall, N. A., and Trivelpiece, A. W., 1973, Principles of Plasma Physics (McGraw-Hill).

Lau, Y. Y., 1982, Simple macroscopic theory of cyclotron maser instabilities. IEEE Trans. Electron Devices, ED-29, 320-335.

Lau, Y. Y., Chu, K. R., Barnett, L. R., and Granatstein, V. L., 1981, Gyrotron travelling wave amplifier: I. analysis of oscillations. Int. J. Infrared and Millimeter Waves, 2, 373-393.

Lin, A. T., 1984, Doppler shift dominated cyclotron masers. Int. J. Elect., 57, 1097-1107.

Lin, A. T., and Lin, C.- C., 1985, Doppler-shift dominated cyclotron maser amplifiers. Int. J. Infrared and Millimeter Waves, 6, 41-51.

Ott, E. and Manheimer, W. M., 1975, The theory of microwave emission by velocity-space instabilities of an intense relativistic electron beam. IEEE Trans. Plasma Science, PS-3, 1-5.

Petelin, M. I., 1974, On the theory of ultrarelativistic cyclotron self-resonance masers. Izv. VUZov Radiofizika, 17, 902-908 [Radiophysics and Quantum Electronics, 17, 686-690].

Schneider, J., 1959, Stimulated emission of radiation by relativistic electrons in a magnetic field. Phys. Rev. Lett., 2, 504-505.

Sprangle, P. and Drobot, A. T., 1977, The linear and self-consistent nonlinear theory of the electron cyclotron maser instability. IEEE Trans. on Microwave Theory and Techniques, MTT-25, 528-544.

Sprangle, P. and Manheimer, W. M., 1975, Coherent nonlinear theory of a cyclotron instability. Physics of Fluids, 18, 224-230.

Sprangle, P., Tang, C. M., and Serafim, P., 1985, Induced Resonance electron cyclotron (IREC). Proc. Seventh Int. FEL Conf. Tahoe City, CA, Sept. 8-13.

Twiss, R.Q., 1958, Radiation transfer and the possibility of negative absorption in radio astronomy. Aust. J. Phys., 11, 564-579.

Vitello, P., 1984, Cyclotron maser and peniotron-like instabilities in a whispering gallery mode gyrotron. IEEE Trans. on Microwave Theory and Techniques, MTT-32, 917-921.

Vomvoridis, J. L., 1982, An efficient Doppler-shifted electron-cyclotron maser oscillator. Int. J. Elect., 53, 555-571.

Zhang, S.- C., 1985, Kinetic theory of Traveling wave gyro-peniotron. Int. J. of Infrared and Millimeter Waves, 6, 1217-1235.

Table I: 100 GHz CARM Oscillator Parameters

Electron Beam Energy	600 kV
Optimum Beam Current	250 Amp
Threshold Current	60 Amp
Initial Transverse Velocity	0.46c
Initial Axial Velocity	0.76c
Operating Mode	$TE_{10,1}$
Cavity Length	4.6 cm
Cavity Wall Radius	1.2 cm
Annular Beam Radius	1.1 cm
Wave Phase Velocity	1.13c
Cavity Output Reflectivity	0.9
Cavity Q	2200
Magnetic Field	23 kG
Interaction Efficiency	25 %
Output Power	37 MW

Table II: 94 GHz CARM Amplifier Parameters

Electron Beam Energy	1 MeV
Optimum Beam Current	500 Amp
Initial Transverse Velocity	0.33c
Initial Axial Velocity	0.76c
Operating Mode	TE_{11}
Interaction Length	54.5 cm
Waveguide Wall Radius	0.54 cm
Solid Beam Radius	0.3 cm
Wave Phase Velocity	1.015c
Magnetic Field	13.2 kG
Saturated Efficiency	22 %
Output Power	110 MW
Small Signal Bandwidth (FWHM)	10 %
Large Signal Bandwidth (FWHM)	3 %

Table III: 2 THz Second Harmonic CARM Amplifier Parameters

Electron Beam Energy	1.2 MeV
Optimum Beam Current	1 kA
Initial Transverse Velocity	0.3c
Initial Axial Velocity	0.9c
Operating Mode	$TE_{10,1}$
Interaction Length	134 cm
Waveguide Wall Radius	0.5 cm
Annular Beam Radius	0.4 cm
Wave Phase Velocity	1.0016c
Magnetic Field	115 kG
Saturated Efficiency	19 %
Output Power	223 MW
Large Signal Bandwidth (FWHM)	0.04 %
Average gain rate	0.4 dB/cm

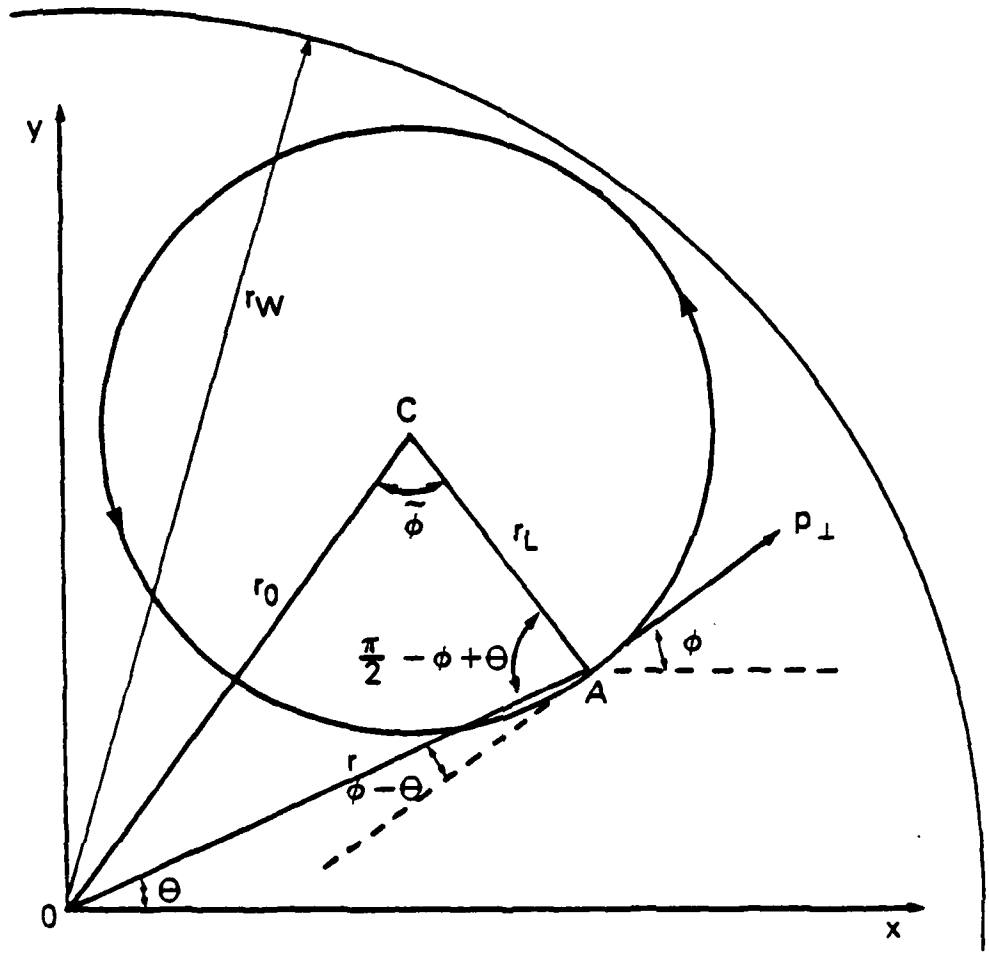

Figure 1: Geometry of interaction.

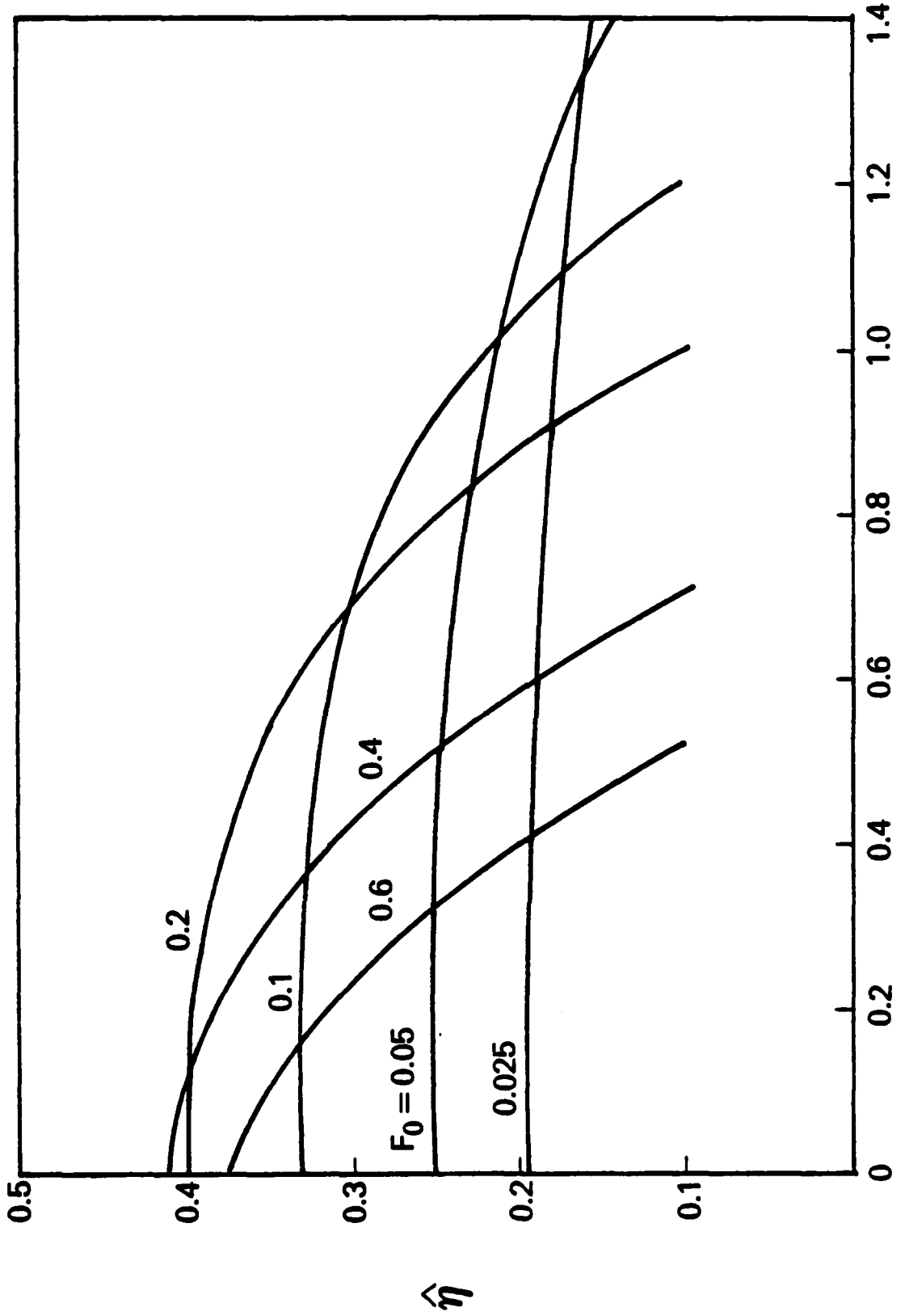

Figure 2: First harmonic (s=1) normalized efficiency versus b for optimized Δ and μ.

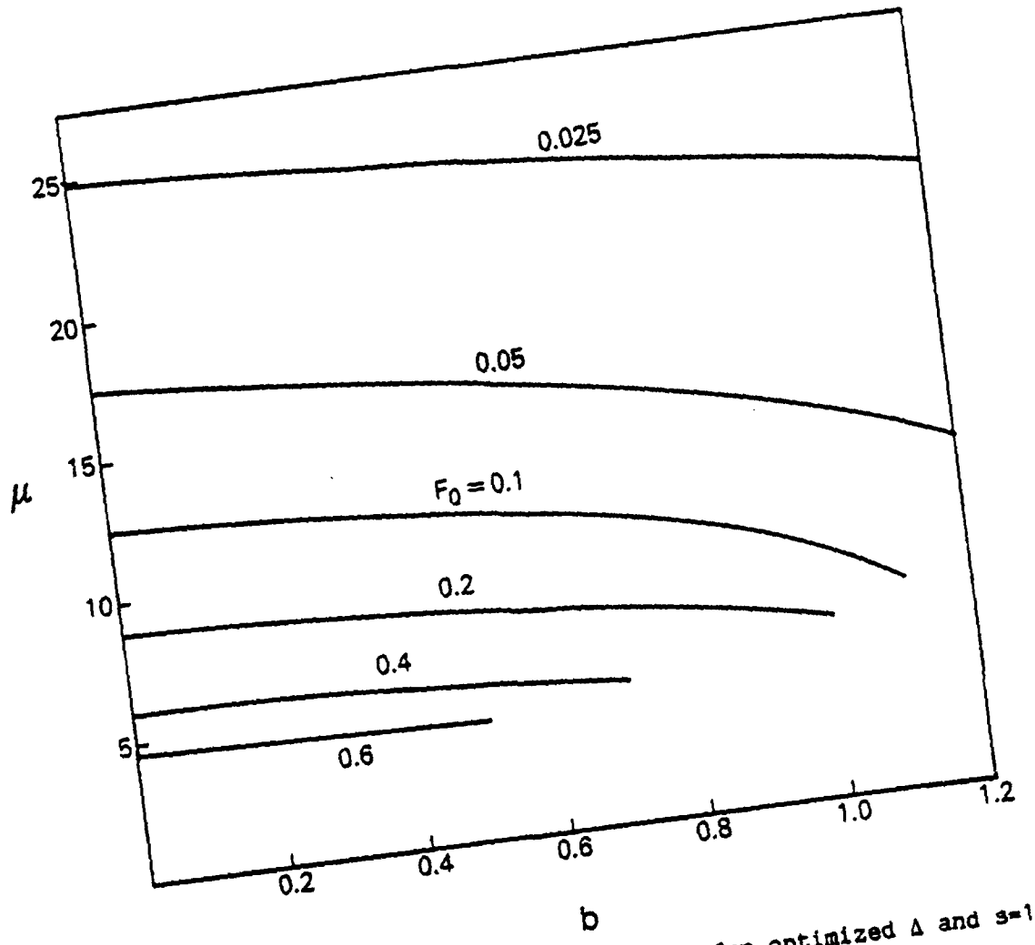

Figure 3: Optimum interaction length versus b for optimized Δ and s=1.

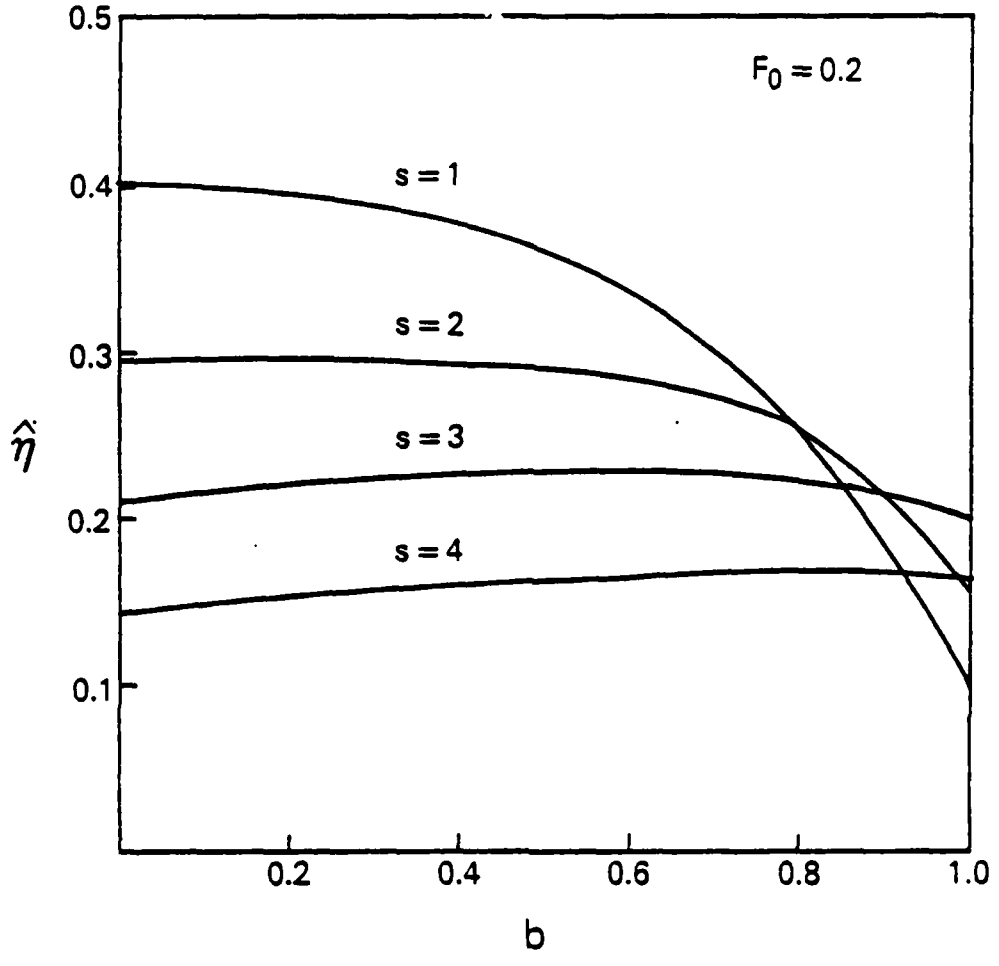

Figure 4: Normalized efficiency of the first four harmonics versus b for $F_o = 0.2$ and optimized Δ and μ.

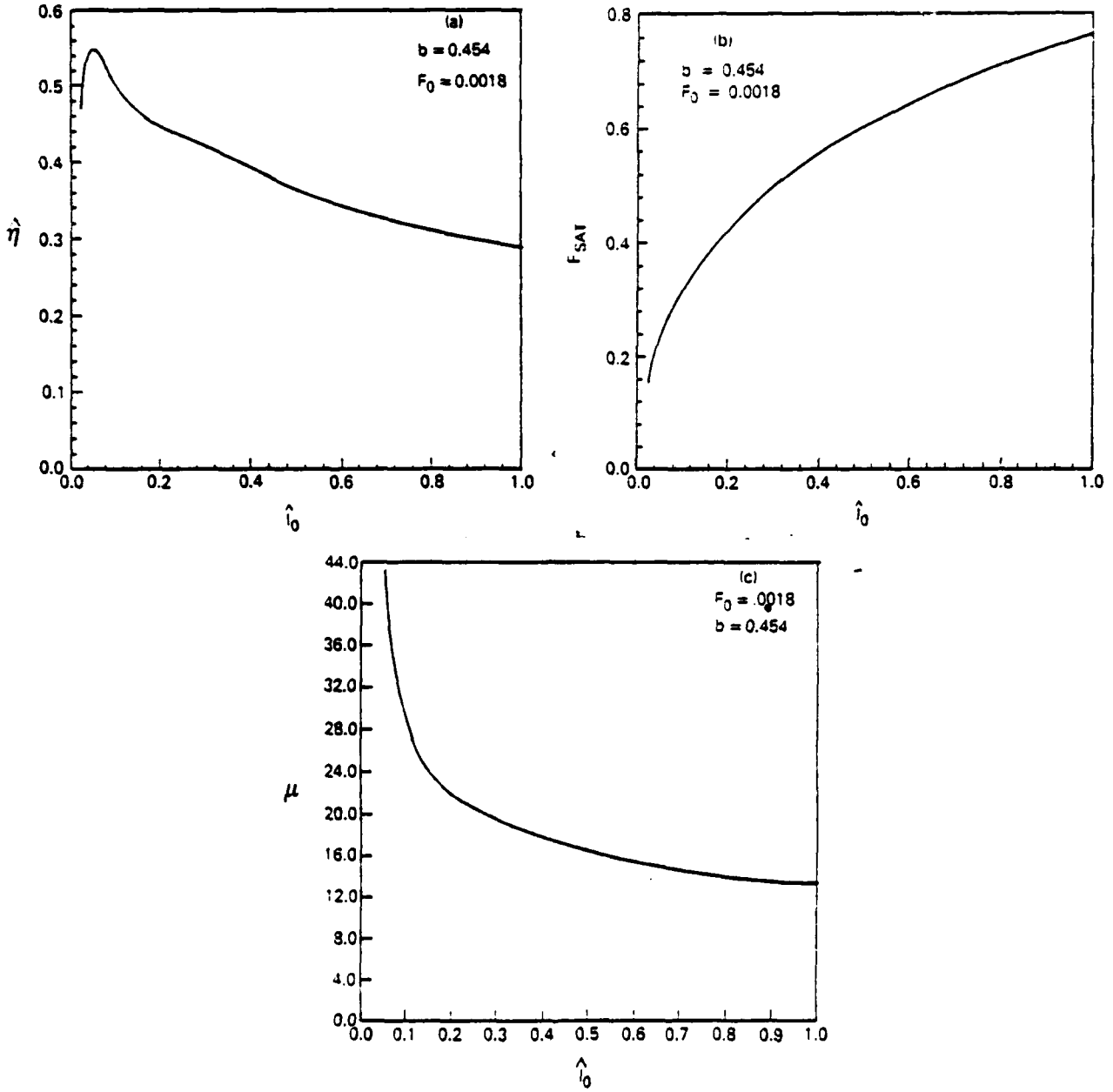

Figure 5: a) Normalized efficiency for first harmonic as a function of normalized current for b = 0.454 and F_0 = 0.0018. The results have been optimized with respect to Δ and interaction length μ . b) Peak normalized wave amplitude corresponding to efficiency shown in a). c) Optimum interaction length corresponding to efficiency shown in a).

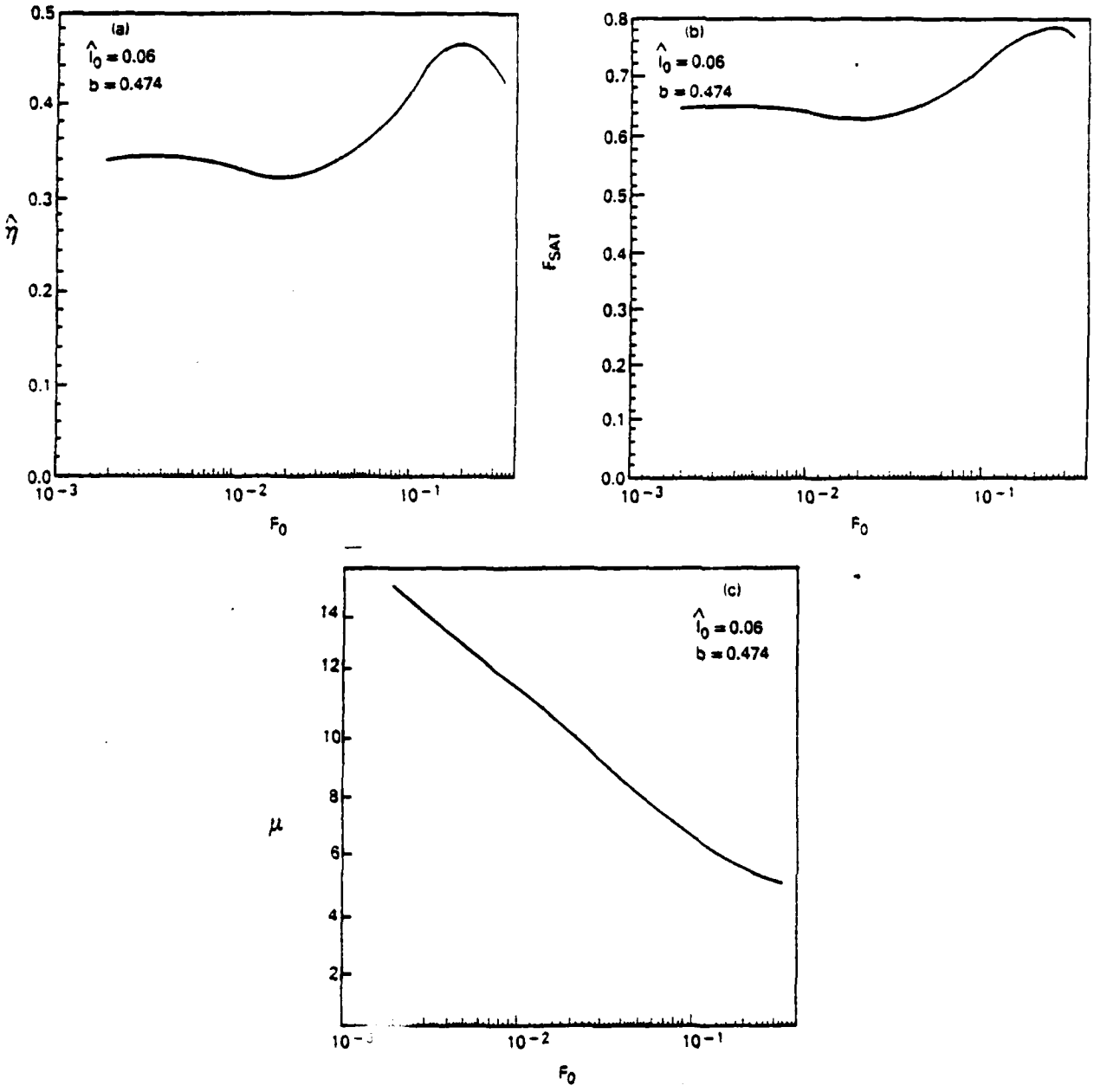

Figure 6: a) Normalized efficiency dependence on the input wave amplitude for the first harmonic (s=1). The normalized current is $\hat{I}_o$ = 0.60 and b = 0.47. The results have been optimized with respect to Δ and μ as in Figure 5. The optimum values of saturation wave amplitude and interaction length are shown in b) and c).

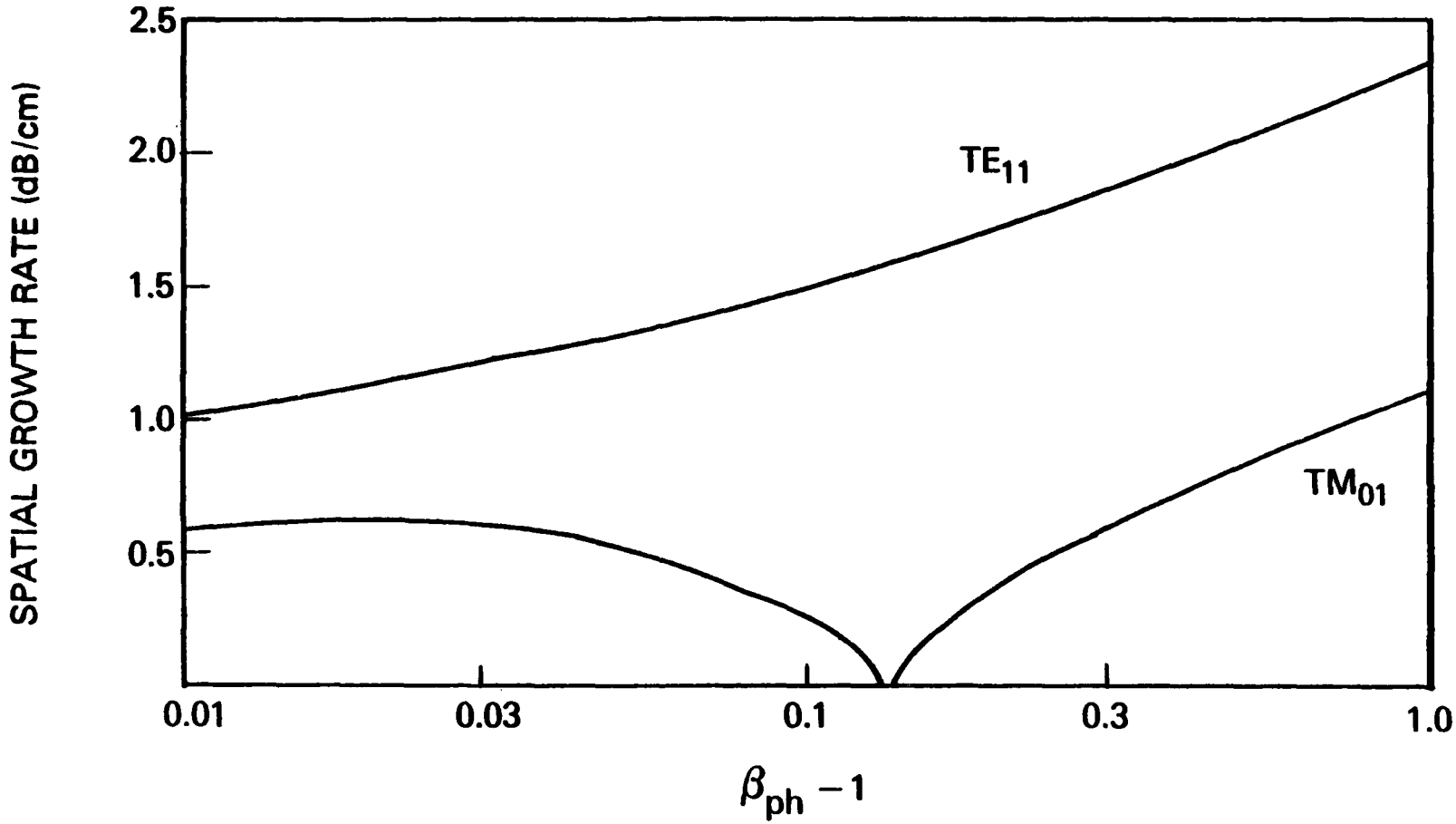

Figure 7: Comparison of the first harmonic (s=1) small signal spatial growth rates for the TE_{11} and TM_{01} modes as a function of phase velocity (and frequency) in the design waveguide (r_w = 0.54 cm).

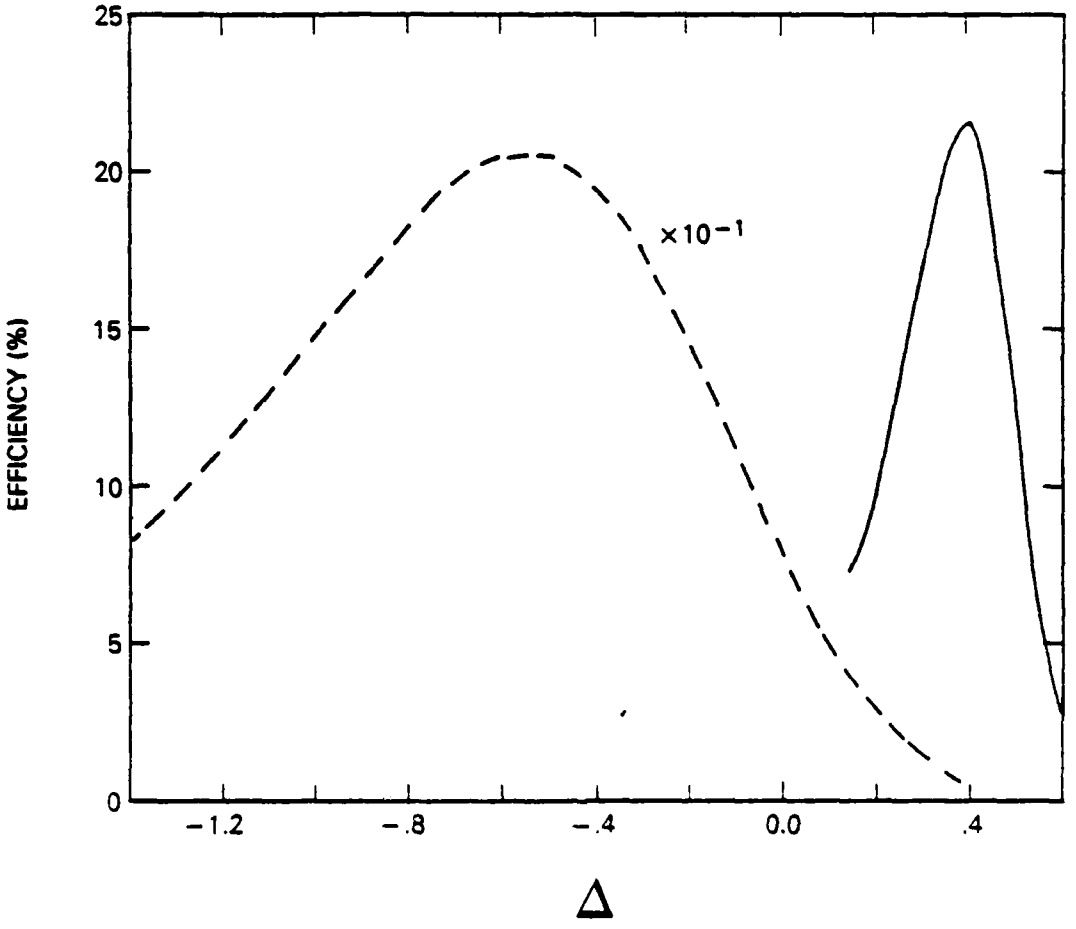

Figure 8: The small signal (dashed curve) and nonlinear (solid curve) first harmonic efficiencies plotted as a function of the detuning parameter Δ. The interaction parameters are given in Table II. The small signal curve has been multiplied by a factor of 10 for clarity.

END

10-86

DTIC